Article

Redundant roles of the phosphatidate phosphatase family in triacylglycerol synthesis in human adipocytes

Ana Temprano[1,2], Hiroshi Sembongi[3*], Gil-Soo Han[4], David Sebastián[5,6,7], Jordi Capellades[7,8], Cristóbal Moreno[1,7], Juan Guardiola[9], Martin Wabitsch[10], Cristóbal Richart[1,11], Oscar Yanes[7,8,12], Antonio Zorzano[5,6,7], George M. Carman[4], Symeon Siniossoglou[3], Merce Miranda[1,7]

[1] Joan XXIII University Hospital, Pere Virgili Health Research Institut (IISPV), Modular Building, C/ Mallafre Guasch, Tarragona 43005, Spain
[2] Department of Biochemistry and Molecular Biology, Rovira i Virgili University, Tarragona, Spain
[3]Cambridge Institute for Medical Research, University of Cambridge Wellcome Trust/Medical Research Council Building, Hills Road, Cambridge CB2 0XY, UK
[4] Department of Food Science and the Rutgers Center for Lipid Research, New Jersey Institute for Food, Nutrition and Health, Rutgers University, New Brunswick, NJ, USA
[5] Institute for Research in Biomedicine (IRB Barcelona), The Barcelona Institute of Science and Technology, Barcelona, Spain
[6] Department of Biochemistry and Molecular Biology, Faculty of Biology, University of Barcelona, Barcelona, Spain
[7] Biomedical Research Networking Centre in Diabetes and Associated Metabolic Disorders (CIBERDEM), Instituto de Salud Carlos III, Madrid, Spain
http://www.ciberdem.org/
[8] Centre for Omic Sciences, Rovira i Virgili University, Reus, Spain
[9] Department of Pulmonary, Critical Care and Sleep Medicine, University of Louisville, Louisville, KY, USA
[10] Division of Paediatric Endocrinology and Diabetes, Interdisciplinary Obesity Clinic, University Clinic for Child and Adolescent Medicine, University of Ulm, Ulm, Germany
[11] GEMMAIR Research Group – Applied Medicine, Department of Medicine and Surgery, Rovira i Virgili University (URV), Tarragona, Spain
[12] Department of Electronic Engineering, Rovira i Virgili University, Tarragona, Spain

Corresponding authors: Merce Miranda, Hospital Universitario Joan XXIII, Instituto de Investigación Biomédica Pere Virgili (IISPV), Edificio Modular, C/ Mallafre Guasch, Tarragona 43005, Spain
Email: mmg@mercemiranda.net

Symeon Siniossoglou, Cambridge Institute for Medical Research, University of Cambridge Wellcome Trust/Medical Research Council Building, Hills Road, Cambridge CB2 0XY, UK
Email: ss560@cam.ac.uk

[*]Present address: Chesterford Research Park, Little Chesterford, Saffron Walden, Essex CB10 1XL, UK.

Received: 22 April 2016 / Accepted: 23 May 2016

Abstract

Aims/hypothesis In mammals, the evolutionary conserved family of Mg^{2+}-dependent phosphatidate phosphatases (PAP1), involved in phospholipid and triacylglycerol synthesis, consists of lipin-1, lipin-2 and lipin-3. While mutations in the murine *Lpin1* gene cause lipodystrophy and its knockdown in mouse 3T3-L1 cells impairs adipogenesis, deleterious mutations of human *LPIN1* do not affect adipose tissue distribution. However, reduced *LPIN1* and PAP1 activity has been described in participants with type 2 diabetes. We aimed to characterise the roles of all lipin family members in human adipose tissue and adipogenesis.

Methods The expression of the lipin family was analysed in adipose tissue in a cross-sectional study. Moreover, the effects of lipin small interfering RNA (siRNA)-mediated depletion on in vitro human adipogenesis were assessed.

Results Adipose tissue gene expression of the lipin family is altered in type 2 diabetes. Depletion of every lipin family member in a human Simpson–Golabi–Behmel syndrome (SGBS) pre-adipocyte cell line, alters expression levels of adipogenic transcription factors and lipid biosynthesis genes in early stages of differentiation. Lipin-1 knockdown alone causes a 95% depletion of PAP1 activity. Despite the reduced PAP1 activity and alterations in early adipogenesis, lipin-silenced cells differentiate and accumulate neutral lipids. Even combinatorial knockdown of lipins shows mild effects on triacylglycerol accumulation in mature adipocytes.

Conclusions/interpretation Overall, our data support the hypothesis of alternative pathways for triacylglycerol synthesis in human adipocytes under conditions of repressed lipin expression. We propose that induction of alternative lipid phosphate phosphatases, along with the inhibition of lipid hydrolysis, contributes to the maintenance of triacylglycerol content to near normal levels.

Keywords: Basic science, Cell lines, Human, Lipid metabolism

Abbreviations

DAG	Diacylglycerol
DNL	De novo lipogenesis
ER	Endoplasmic reticulum
FAO	Fatty acid oxidation
LPP	Lipid phosphate phosphatases
ORO	Oil Red O staining
PAP	Phosphatidate phosphatase
PPAR	Peroxisome proliferator activated receptor
SGBS	Simpson–Golabi–Behmel syndrome
siRNA	Small interfering RNA
SAT	Subcutaneous adipose tissue
TAG	Triacylglycerol
VAT	Visceral adipose tissue

Introduction

Triacylglycerols (TAGs) are neutral lipids that act as the major energy storage molecules, repository for fatty acids, and phospholipid precursors [1]. Adipocytes are the specialised cells for neutral lipid storage and one of their important physiological functions is to buffer the toxicity caused by NEFAs. Excessive calorie intake or genetic disorders can lead to lipid deposition in ectopic tissues, impair their function and lead to dyslipidaemia, insulin resistance and type 2 diabetes [2-3].

Lipins are Mg^{2+}-dependent phosphatidate phosphatases (PAP1) with a central role in lipid metabolism, and catalyse the dephosphorylation of phosphatidate to diacylglycerol (DAG), which can be (1) acylated to form TAG, or (2) used in phospholipids synthesis [4-5]. A second type of PAP activity is mediated by Mg^{2+}-independent transmembrane lipid phosphate phosphatases (LPPs, also known as PAP2), which are thought to regulate signalling properties of phosphatidate and DAG [6].

Fungi, nematodes and insects express one lipin, whereas mammals express three paralogues called lipin-1, -2 and -3 that exhibit distinct but overlapping expression in many mouse and human tissues [5]. Consistent with their key metabolic role, loss of lipin function disrupts TAG production, membrane organisation and phospholipid synthesis in several model organisms [7]. Interestingly, besides their enzymatic functions, lipins also regulate transcription [8-13]. For instance, lipin-1 transcriptional co-regulation of the peroxisome proliferator activated receptor (PPAR)A/PPAR coactivator 1α axis modulates fatty acid oxidation (FAO) in liver [9].

Lpin1 gene was originally identified as the deficient gene causing lipodystrophy, insulin resistance, peripheral neuropathy and neonatal fatty liver in the *fld* (also known as *Lpin1*) mouse model [14]. Loss of lipin-1 in mice blocks adipogenesis at an early stage preceding TAG accumulation, suggesting a distinct role of lipin-1 in

differentiation [15-16]. Consistently, small interfering RNA (siRNA)-mediated silencing of lipin-1 in mouse 3T3-L1 cells potently inhibits adipogenesis [10, 17]. In contrast, deleterious mutations in the *LPIN1* gene in humans, which lead to recurrent rhabdomyolysis in childhood, do not compromise adipose tissue [18]. The basis of this difference between mice and humans is unknown; it has been hypothesised that it is due to compensation by the other two lipins [18]. Nevertheless, genetic variation in *LPIN1* and *LPIN2*, and reduced *LPIN1* expression levels and PAP1 activity in human adipose tissue have been associated with type 2 diabetes [19-25], which suggests a loss of their protective role against lipotoxicity.

While most of the studies have been performed on mice, very little is known on the roles of lipin-1 in human adipocyte physiology, while there is virtually no information on lipin-2 and -3. This prompted us to investigate the functions of the three lipins in type 2 diabetes and in human adipocytes by studying the effects of loss-of-function.

Methods

Reagents Unless otherwise stated, all reagents were supplied by Sigma-Aldrich Corporation (St Louis, MO, USA). Human insulin was purchased from NovoNordisk (Bagsværd, Denmark); rosiglitazone from Cayman Chemical (Ann Arbor, MI, USA); and cell culture media from Gibco (Thermo Fisher Scientific, Waltham, MS, USA).

Human adipose tissue biopy collection The cross-sectional study has been previously described [26, 27]. We used a cohort of 71 participants for the gene expression analysis, and of 28 males for protein analysis. They were grouped as: (1) normoweight (BMI between 18.50 and 24.99), (2) obesity (BMI ≥25) and (3) obesity with type 2 diabetes (hereafter type 2 diabetes). Group characteristics are described in Electronic Supplementary Material (ESM) Table 1A and 1B, respectively. Samples were obtained at the Joan XXIII University Hospital (Tarragona, Spain). VAT and SAT samples (gene expression) and SAT samples (protein expression) were obtained during abdominal elective surgical procedures for benign pathologies (cholecystectomy or surgery for abdominal hernia). The Ethics Committee approved the study and informed consent was obtained from all participants. Participants had no systemic disease other than obesity [28] or type 2 diabetes [29]. See ESM Methods for further details.

Cell culture and differentiation Simpson–Golabi–Behmel syndrome (SGBS) cells, a well-established system for studies of human adipocyte biology [30, 31], were differentiated as described [30], except that 1 nmol/l of insulin, 0.1 μmol/l cortisol, 2 μmol/l rosiglitazone and 25 nmol/l dexamethasone were used. See ESM Methods for detailed information.

Adipose-derived stem cells were isolated from adipose tissue (n=3 female donors; age (years) 37.4±6.4, BMI (kg/m2) 25.9±3.0) from patients undergoing elective liposuction surgery. See ESM Methods for the isolation, proliferation and adipogenic procedure details.

Quantification of expression levels Protein content in cell lysates (lysis buffer: 50 mmol/l HEPES pH 7.4, 150 mmol/l NaCl, 4 mmol/l $MgCl_2$, 1% Triton X-100 and protease inhibitors) was quantified by using the bicinchoninic acid assay (Pierce, Rockford, IL, USA). See ESM for western blot procedures. Antibodies against lipin family members were previously described [17, 32]. Quantitative PCR was performed as previously described [28], and expressed relative to cyclophilin A and to control. See ESM for detailed information and ESM Table 2B and 2C for commercial reagents.

Cell Fractionation For cell fractionation, SGBS cells were grown and differentiated until day 10. Subcellular fractions were obtained by using hypotonic lysis followed by high salt extraction of nuclei. See ESM Methods for further details.

Gene silencing Transfections of SGBS cells with siRNA oligonucleotides were carried out by using Lipofectamine RNAiMAX transfection reagent (Thermo Fisher Scientific). Pre-adipocyte knockdowns were performed as a two-shots transfection of a mix of two siRNA duplexes per gene (12.5 nmol/l of each duplex) (see ESM Table 2A): reverse transfection at the start of the experiment and forward transfection the day before confluence. The non-targeting control concentration depended on total siRNA amount of the single and multiple knockdowns.

Neutral lipid accumulation and metabolism Data were obtained from differentiated SGBS cells and normalised by protein content. For TAG analysis, cells were processed as previously described [32], except that the supernatant fraction was analysed with the Serum Triglyceride Determination kit (Sigma). Glycerol release to cell culture media was quantified by using the Free Glycerol Determination Kit (Sigma). Fatty acid and glucose incorporation into TAGs, and FAO analysis were performed as previously described [33], with slight modifications (see ESM Methods for details).

Enzyme assay Cell lysates (lysis buffer: 50 mmol/l Tris-HCl pH 7.5, 0.25 mol/l sucrose, 10 mmol/l 2-mercaptoethanol, protease inhibitors) were subjected to centrifugation at 1,000 *g* for 10 min at 4°C to remove cell debris. Protein concentration was determined by the method of Bradford [34] using BSA as a reference protein. Preparation of the substrate and measure of PAP activity was as previously described [35-37]. See ESM Methods for details. The Mg^{2+}-independent LPP activity was measured in the same reaction mixture except that 2 mmol/l EDTA was substituted for 0.5 mmol/l $MgCl_2$. The Mg^{2+}-dependent PAP1 activity was determined by subtraction of LPPs activity from PAP activity. A unit of PAP activity (expressed as units/mg protein) was defined as the amount of enzyme catalysing the formation of 1 nmol of product/min.

Metabolomic analysis—SGBS cells were grown, transfected with siRNA as explained above, and differentiated to day 4. In brief, lipids were extracted from lyophilized samples by using dichloromethane/methanol and water. The organic phase (lipidic) was collected, dried under a stream of nitrogen, and resuspended in acetonitrile/isopropanol/water for untargeted LC-MS analysis. Differentially regulated

lipids (p value<0.05 and fold>2) were retained for compound identification by MS/MS analyses. See ESM Methods for detailed procedures.

Statistical analysis Statistical analysis was performed by using the SPSS software version 15 (Chicago, IL, USA). ANOVA, Kruskal–Wallis, Pearson χ^2, Spearman correlation and Linear Stepwise Regression tests were performed for the human cohort analysis, and the General Linear Model Univariate test and Student T-test for in vitro experiments. Statistical power in the cohort analysis was ≥80%. The level of significance was set at α=0.05.

Results

Adipose tissue expression levels of the lipin family is altered in type 2 diabetes To investigate the roles of lipin paralogues in adipose tissue, we started by examining their gene expression in paired abdominal subcutaneous (SAT) and visceral (VAT) adipose tissue biopsies. As shown in Fig. 1a–c and ESM Fig. 1a–c, *LPIN1* expression was reduced in both SAT ($p<0.001$) and VAT ($p=0.021$) in the obesity and type 2 diabetes groups compared with normoweight. *LPIN2* expression was similar among groups. In contrast, SAT *LPIN3* expression was significantly increased in the type 2 diabetes ($p=0.018$). At the protein level, SAT showed only lipin-1 was downregulated in obesity and in type 2 diabetes compared with normoweight ($p=0.034$) (Fig. 1d–f).

Correlation analysis showed a negative association of *LPIN1* expression levels with BMI, HOMA-IR and plasma TAG levels. In contrast, expression of *LPIN3* positively correlates with fasting glucose (SAT) and NEFA (VAT) (Table 1). Regression analysis was performed, assessing age and sex as confusing and interacting variables, and showed that (1) SAT *LPIN1* expression depends negatively on HOMA-IR ($R=0.466$, $p=0.005$, excluded variables: BMI, TAG, age and sex; $LPIN1_{SAT} = 0.37\times\log_{10}\text{HOMA}+0.984$), and (2) SAT *LPIN3* expression depends positively on plasma glucose levels ($R=0.414$, $p=0.002$, excluded variables: age and sex; $LPIN3_{SAT} = 1\times10^{[1.202\times\log_{10}\text{Glucose}-0.961]}$).

The observed changes of the lipin family expression in type 2 diabetes participants may account for the altered PAP1 activity in adipocytes from these patients. Moreover, *LPIN3* expression is associated with fasting glucose levels. Alterations in lipin-3 protein levels in SAT of participants with type 2 diabetes may be masked by its presence also in the stromal vascular fraction (data not shown).

The three lipin family members have a role in early human adipogenesis Next, we examined the expression of lipins during adipogenesis. Lipin-1 was induced, and lipin-2 and lipin-3 levels were present along SGBS adipogenesis with slight variation (Fig. 2a,b). Thus, SGBS adipocytes, similar to differentiated adipose-derived stem cells (ESM Fig. 1d), express the three lipin paralogues. Finally, under baseline conditions, the three lipins partitioned between the cytosolic, intranuclear and membrane-bound forms in SGBS adipocytes (ESM Fig. 1e).

To address the effects of decreased PAP1 activity on adipogenesis, we depleted each lipin member prior to the induction of adipogenesis in SGBS pre-adipocytes (by using siRNA; see Methods and Fig. 2c). Cells were analysed at day four after differentiation to assess adipogenic early events. Protein expression analysis was used to confirm knockdowns and evaluate possible compensatory mechanisms among lipins. Lipin-1 depleted cells responded by compensatory upregulation of lipin-2 protein (Fig. 2d and ESM Fig. 1f), but not *LPIN2* transcript levels (data not shown). Conversely, single lipin-2 and lipin-3 knockdowns led to lower protein levels of the other family members (Fig. 2d). Analysis of PAP1 activity showed that lipin-1 accounted for almost all PAP1 activity (lipin-1-depleted cells showed 5% of PAP1 activity in the control), with lipin-2 and lipin-3 single knockdowns reducing it to 49% and 61%, respectively (Fig. 2e).

Next, we analysed incorporation of fatty acids and glucose into TAGs. While esterification of fatty acids was downregulated in lipin-1- and lipin-2-depleted cells, glucose incorporation into TAGs decreased in all three lipin-depleted cells (Fig. 2f).
Finally, we analysed the expression levels of transcription factors that promote early adipogenesis. *CEBPA* was downregulated in cells depleted of any lipin family member, and *CEBPB* was decreased upon lipin-2 deficiency (Fig. 2g). Under these conditions,

gene expression of two key transcription factors regulated by CCAAT/enhancer binding proteins, *PPARG* and *SREBP1* were downregulated (Fig. 2g), and also at the protein level (ESM Fig. 2a,b). *CEBPD* showed a significant upregulation in cells depleted of any lipin family member (Fig. 2g), probably due to the triggering of a compensation mechanism.

Given the role of lipins in neutral lipid biosynthesis, we next explored expression of lipogenic genes. The expression of these genes was significantly downregulated in cells depleted of any lipin family member (Fig. 2h). In contrast, glycerol-3-phosphate acyltransferase was significantly upregulated in the lipin-1 and lipin-2 knockdowns (Fig. 2h). Lipid quantification by mass spectrometry showed that, among the lipid species that were altered, the levels of most DAG (ESM Fig. 2c) and TAG (ESM Fig. 2d) species were downregulated in cells depleted of any lipin compared with controls. Interestingly, phosphatidate levels did not change (data not shown).

Overall, despite the crosstalk between lipin family members, lipin-1 silencing leads to a 95% depletion of PAP1 activity. However, our results point to a role of all three members on early stages of human adipogenesis.

Single lipin silencing does not block TAG accumulation in fully differentiated adipocytes Next, we analysed the effects of lipin silencing in SGBS pre-adipocytes on late adipogenesis. Similarly to the above experiments, we depleted each lipin member prior to induction of adipogenesis in SGBS pre-adipocytes, and cells were analysed at day 10 after differentiation (Fig. 3a), where protein downregulation of lipins still persisted (Fig. 3b and ESM Fig. 3a).

At day 10, lipin-1 depleted cells still responded by compensatory upregulation of lipin-2 protein (Fig. 3b and ESM Fig. 3a). Additionally, both single lipin-2 and lipin-3 knockdowns led to lower protein levels of the other lipins. PAP1 activity analysis showed that lipin-1 accounted for almost all PAP1 activity (lipin-1-depleted cells showed 3% of the activity in the control). Lipin-2 and lipin-3 single knockdowns reduced PAP1 activity only slightly (84% and 74%, respectively) (Fig. 3c).

Next, we assessed neutral lipid accumulation. Depletion of any lipin triggered a slight reduction (15% to 34%) in TAG accumulation (Fig. 3d). Expression of key transcription factors for lipogenesis (ESM Fig. 3a,b) and genes of lipid biosynthesis (ESM Fig. 3c) were altered to a lesser extent compared with the effects observed at day four.

Finally, fatty acid esterification into TAGs and α-glycerophosphate synthesis/de novo lipogenesis (DNL) were downregulated in cells depleted of any lipin (Fig. 3e). Compared with day 4, lipin-3 depletion also showed reduced fatty acid esterification into TAGs at day 10.

Overall, the effects of lipin knockdown were mild on fully differentiated adipocytes suggesting that cells overcame the initial impairment of lipid gene expression. This may be due to the existence of enough remnant protein amounts of lipins, although PAP1 activity at day 10 was still almost absent in the lipin-1 knockdowns.

Combinatorial silencing of lipins does not further alter the phenotype of fully differentiated adipocytes We then asked whether compensation by other lipin family members might help cells to recover the initial alterations shown at day 4 after adipogenesis. We used a combinatorial knockdown to deplete combinations of two of

the three lipins in SGBS pre-adipocytes (see Methods), and analysed cells at day 10 of differentiation (as in Fig. 3a).

Double lipin-1 and lipin-3 knockdowns led to an upregulation of lipin-2 protein levels (Fig. 4a and ESM Fig. 4). This compensatory pattern hindered the efficiency of lipin-2 knockdown in the double (lipin-1 and -2) and triple knockdown cells. Nevertheless, PAP1 activity in the triple knockdown was residual compared with the control (0.18±0.31 vs 39.29±3.42 nmol min^{-1} mg^{-1}).

Despite the almost complete lack of PAP1 activity, neutral lipid accumulation was not totally compromised in the triple knockdown (Fig. 4b). This is in agreement with the fact that deleterious mutations in *LPIN1* do not affect adipose tissue development in humans, and it suggests that it is unlikely to be due to a compensatory upregulation of lipin-2 (Fig. 2d), since the double lipin-1 and -2 knockdown shows a similar reduction in the content of neutral lipids (Fig. 3d and 4b).

Moreover, depletion of the three lipins did not significantly affect fatty acid esterification into TAGs and only slightly downregulated α-glycerophosphate synthesis/DNL (Fig. 4c), pointing to an improvement compared with day 4 (day 4 incorporation of fatty acids: 0.52 ± 0.35, $p=0.006$, and of glucose: 0.32 ± 0.15, $p<0.001$, fold over the control level).

Consumption of TAGs is reduced in lipin-depleted SGBS adipocytes Lipid droplets accumulate neutral lipids in a dynamic manner, with a balance among lipid biosynthesis, lipid hydrolysis and FAO in mitochondria. To test whether cells protect intracellular lipids by reducing its consumption, we analysed the rates of palmitate oxidation. The results show similar FAO rates in the control, single (Fig. 5a) and triple knockdown (Fig. 5b). In contrast, levels of glycerol release were downregulated

compared with controls in the single (Fig. 5c), and in all combinatorial knockdowns (Fig. 5d). Thus, reduced consumption may contribute to the accumulation of neutral lipids in lipin-depleted adipocytes.

The LPP family is upregulated under conditions of repressed lipin expression Next, we tested whether the Mg^{2+}-independent LPPs could provide an alternative pathway for DAG synthesis. LPP activity was highly induced in the lipin-1 single knockdown (3.50±1.18-fold increase over control levels) (Fig. 6a), and in the triple knockdown (2.74±0.97-fold increase) at day 10 of differentiation (Fig. 6b).

Moreover, the expression of *LPP3* (also known as *Plpp3/PPAP2B*) was upregulated in the single (Fig. 6c) and in the combinatorial lipin knockdowns at day 10 (Fig. 6d) and, similarly to lipogenic genes, upregulation was higher at day four (ESM Fig. 5a). This was confirmed by using other commercial sources of lipin-1 siRNA (ESM Fig. 5b) and analysing LPP expression at day four of differentiation (ESM Fig. 5c).

Propranolol, a nonspecific ß-blocker, is an effective PAP1 activity inhibitor and modestly effective as LPP inhibitor, with the LPP3 isoform being more sensitive to inhibition [36]. Propranolol treatment during adipogenesis (Fig. 6e) altered lipogenic gene expression (Fig. 6f) and blocked lipid droplet formation in SGBS adipocytes (ESM Fig. 5d).

Discussion

Herein we have addressed the contribution of the lipin paralogues to human adipogenesis. Decreased lipin expression levels and PAP1 activity in adipose tissue have been linked with insulin resistance [23-25]. In our cohort, adipose tissue expression confirmed that lipin-1 is altered in type 2 diabetes and that *LPIN1* is negatively associated with insulin resistance. Moreover, we show that *LPIN3* transcript levels are positively related with fasting glucose levels. This prompted us to analyse separately the effects of gene silencing of each lipin paralogue in adipogenesis.

Previous studies have established that lipin-1 plays a major role in fat metabolism in rodents, with lipin-1 deficiency causing lipodystrophy features in mice and rats [14, 38]. The role of lipins in human adipogenesis is still undefined: mutations in the *LPIN1* gene have not yet been detected in human lipodystrophy [39-40]. Moreover, deleterious *LPIN1* mutations cause paediatric rhabdomyolysis while fat distribution, average weight and plasma biochemical variables are normal [18]. Our data suggest that the lack of an essential role for PAP1 activity in human adipogenesis is not due to compensation by lipin-2 or lipin-3. We find that the triple lipin silencing in SGBS pre-adipocytes maintains the ability to incorporate fatty acids into TAG and accumulate neutral lipids despite loss of nearly all PAP1 activity.

SGBS pre-adipocytes are differentiated in the absence of serum and, therefore, neutral lipids should be obtained from DNL. Besides, although glyceroneogenesis is the major pathway for glycerol synthesis in the mature adipocyte [41], during adipogenesis glycolysis may account for an important source of α-glycerophosphate. Thus, glucose incorporation into TAGs may account for DNL, but also for α-glycerophosphate synthesis via glyceroneogenesis and glycolysis. Downregulated α-glycerophosphate synthesis/DNL points to broader effects of lipin silencing other than TAG synthesis.

Moreover, the putative intranuclear roles of lipin-1, -2 and -3 in SGBS adipocytes add some complexity to the above.

The lipin family members cooperate for optimal PAP activity in mouse adipose tissue [42], liver [43-44], brain [43] and human primary myoblasts [45]. Our data show that human lipin-1 accounts for most PAP1 activity in SGBS adipocytes and that upregulation of lipin-2 in lipin-1-depleted cells does not compensate for PAP1 activity. By contrast, downregulation of PAP1 activity in lipin-2 and lipin-3 single knockdowns cannot be fully attributed to their own depletion since they also downregulate lipin-1.

Activation of non-lipin compensatory pathways may also mask the lipin phenotypes. Nevertheless, (1) we found no evidence, at the mRNA level, of upregulation of the monoacylglycerol *O*-acyltransferase pathway that can generate DAG from monoacylglycerol [46-47] (data not shown); and (2) cholesteryl esters levels are likely not upregulated since the effect of lipin knockdown on neutral lipid content looks similar by Oil Red O staining (ORO) and TAG content (ORO: 0.76 ± 0.06, and TAG: 0.85 ± 0.13 in the lipin-1 knockdown, and ORO: 0.74 ± 0.12, and TAG: 0.54 ± 0.33 in the triple lipin knockdown, compared with the control set as 1). In contrast, LPP activity was induced in the lipin knockdowns, possibly due to an earlier upregulation of their transcript levels (observed by day four). Moreover, inhibition of both lipins and LPPs with propranolol completely blocked lipid droplet formation, although this fact must be taken with caution because of the non-specificity of this compound. LPPs hydrolyse phosphatidate as well as different substrates, and act on the outer surface of plasma membrane and in the luminal surface of endoplasmic reticulum (ER) and Golgi membranes [6] and thus, it is not clear if they can have access to the phosphatidate formed from glycerol phosphate and acyl-CoA. However, in yeast, TAG synthesised

both in the cytosolic and luminal leaflets of the ER membranes are efficiently packed into lipid droplets [48].

Another strategy to protect the lipid storage when glycerolipid synthesis is compromised might be downregulation of lipid hydrolysis and FAO. Lipin-1 regulates basal lipolysis [46], and modulates FAO transcript expression levels [8]. We show that all combinatorial knockdowns of lipins downregulate basal lipolysis to a greater extent than reduction of neutral lipid content.

In summary, we confirm that adipose tissue expression of the lipin family is altered in type 2 diabetes. Furthermore, loss of nearly all PAP1 activity, due to combined lipin-1, -2 and -3 knockdown, has only mild effects on final adipogenesis and lipid accumulation in SGBS cells. Conversely, lipin-2 and lipin-3 may contribute little to total PAP activity, but still play a role in early adipogenesis. Our results suggest a compensation strategy to accumulate near normal neutral lipid levels, activating other pathways (such as LPPs) and inhibiting TAG hydrolysis. More work is clearly required to decipher whether LPPs or other unknown pathways may compensate lack of PAP1 activity.

Acknowledgements We are grateful to I. Mylonis (Laboratory of Biochemistry, Faculty of Medicine, University of Thessaly, Greece) for advice with the cell fractionation protocol.

Funding This study was supported by research grants from the 'Instituto de Salud Carlos III' (ISCIII, Spanish Ministry of Economy and Competitiveness) (PI10/00967 and CP11/00021 to MM); the R. Barri Private Foundation (PV12142S to MM); the Medical Research Council (G0701446 to SS); and National Institutes of Health Grant (GM028140 to GMC). CIBER de Diabetes y Enfermedades Metabólicas asociadas (CB07708/0012) is an initiative of the ISCIII. MM acknowledges support from the 'Miguel Servet' tenure track programme (CP11/00021), from the Fondo de Investigación Sanitaria (FIS) co-financed by the European Regional Development Fund (ERDF), and supported by a Salvador de Madariaga Mobility fellowship from the Spanish Ministry of Education (PR2011-0584). AT is the recipient of a FI-DGR fellowship (9015-97318/2012) from the Agència de Gestió d'Ajuts Universitaris i de Recerca (AGAUR). The funders had no role in study design, data collection and analysis, decision to publish, or preparation of the manuscript.

Duality of interest The authors declare that there is no duality of interest associated with this manuscript.

Author contributions SS, AZ and MM were the main contributors in the conception, design and interpretation of the data, and in writing the manuscript. AT, HS, G-SH, DS, JC, CM and MM performed the experiments and data analysis, and revised the manuscript. JG, MW, CR, OY and GMC were responsible for acquisition of data and analysis, and revised the manuscript. All authors had final approval of the submitted and published versions. MM is the guarantor of this work and, as such, had full access to all the data in the study and takes responsibility for the integrity of the data and the accuracy of the data analysis.

References

1. Athenstaedt K, Daum G (2006) The life cycle of neutral lipids: synthesis, storage and degradation. Cell Mol Life Sci 63:1355-1369
2. Unger RH (2002) Lipotoxic diseases. Annu Rev Med 53:319-336
3. Huang-Doran I, Sleigh A, Rochford JJ, O'Rahilly S, Savage DB (2010) Lipodystrophy: metabolic insights from a rare disorder. J Endocrinol 207:245-255
4. Han GS, Wu WI, Carman GM (2006) The Saccharomyces cerevisiae Lipin homolog is a Mg2+-dependent phosphatidate phosphatase enzyme. J Biol Chem 281:9210-9218
5. Donkor J, Sariahmetoglu M, Dewald J, Brindley DN, Reue, K (2007) Three mammalian lipins act as phosphatidate phosphatases with distinct tissue expression patterns. J Biol Chem 282:3450-3457
6. Brindley DN, Pilquil C, Sariahmetoglu M, Reue K (2009) Phosphatidate degradation: phosphatidate phosphatases (lipins) and lipid phosphate phosphatases. Biochim Biophys Acta 1791:956-961
7. Harris TE, Finck BN (2011) Dual function lipin proteins and glycerolipid metabolism. Trends Endocrinol Metab 22:226-233
8. Donkor J, Zhang P, Wong S, et al. (2009) A conserved serine residue is required for the phosphatidate phosphatase activity but not the transcriptional coactivator functions of lipin-1 and lipin-2. J Biol Chem 284:29968-29978
9. Finck BN, Gropler MC, Chen Z, et al. (2006) Lipin 1 is an inducible amplifier of the hepatic PGC-1alpha/PPARalpha regulatory pathway. Cell Metab 4:199-210
10. Koh YK, Lee MY, Kim JW, et al. (2008) Lipin1 is a key factor for the maturation and maintenance of adipocytes in the regulatory network with CCAAT/enhancer-binding protein alpha and peroxisome proliferator-activated receptor gamma 2. J Biol Chem 283:34896-34906
11. Liu GH, Gerace L (2009) Sumoylation regulates nuclear localization of lipin-1alpha in neuronal cells. PLoS One 4:e7031
12. Peterson TR, Sengupta SS, Harris TE, et al. (2011) mTOR complex 1 regulates lipin 1 localization to control the SREBP pathway. Cell 146:408-420
13. Kim HB, Kumar A, Wang L, et al. (2010) Lipin 1 represses NFATc4 transcriptional activity in adipocytes to inhibit secretion of inflammatory factors. Mol Cell Biol 30:3126-3139
14. Péterfy M, Phan J, Xu P, Reue K (2001) Lipodystrophy in the fld mouse results from mutation of a new gene encoding a nuclear protein, lipin. Nat Genet 27:121-124
15. Nadra K, Médard JJ, Mul JD, et al. (2012) Cell autonomous lipin 1 function is essential for development and maintenance of white and brown adipose tissue. Mol Cell Biol 32:4794-4810
16. Zhang P, Takeuchi K, Csaki LS, Reue K (2012) Lipin-1 phosphatidic phosphatase activity modulates phosphatidate levels to promote peroxisome proliferator-activated receptor γ (PPARγ) gene expression during adipogenesis. J Biol Chem 287:3485-3494

17. Grimsey N, Han GS, O'Hara L, Rochford JJ, Carman GM, Siniossoglou S (2008) Temporal and spatial regulation of the phosphatidate phosphatases lipin 1 and 2. J. Biol Chem 283:29166-29174

18. Zeharia A, Shaag A, Houtkooper RH, et al. (2008) Mutations in LPIN1 cause recurrent acute myoglobinuria in childhood. Am J Hum Genet 83:489-494

19. Zhang R, Jiang F, Hu C, et al. (2013) Genetic variants of LPIN1 indicate an association with Type 2 diabetes mellitus in a Chinese population. Diabet Med 30:118-122

20. Bego T, Dujic T, Mlinar B, et al. (2011) Association of PPARG and LPIN1 gene polymorphisms with metabolic syndrome and type 2 diabetes. Med Glas Ljek komore Zenicko-doboj kantona 8:76-83

21. Aulchenko YS, Pullen J, Kloosterman WP, et al. (2007) LPIN2 is associated with type 2 diabetes, glucose metabolism, and body composition. Diabetes 56:3020-3026

22. Loos RJ, Rankinen T, Pérusse L, Tremblay A, Després JP, Bouchard C (2007) Association of lipin 1 gene polymorphisms with measures of energy and glucose metabolism. Obesity 15:2723-2732

23. Suviolahti E, Reue K, Cantor RM, et al. (2006) Cross-species analyses implicate Lipin 1 involvement in human glucose metabolism. Hum Mol Genet 15:377-386

24. Yao-Borengasser A, Rasouli N, Varma V, et al. (2006) Lipin expression is attenuated in adipose tissue of insulin-resistant human subjects and increases with peroxisome proliferator-activated receptor gamma activation. Diabetes 55:2811-2818

25. Saggerson ED (1988) Phosphatidate phosphohydrolase: its role in glycerolipid synthesis. CRC Press, Inc., Boca Raton, FL, pp 79 –129

26. Miranda M, Escoté X, Ceperuelo-Mallafré V, et al. (2010) Paired subcutaneous and visceral adipose tissue aquaporin-7 expression in human obesity and type 2 diabetes: differences and similarities between depots. J Clin Endocrinol Metab 95;3470-3479

27. Miranda M, Escoté X, Alcaide MJ, et al. (2010) Lpin1 in human visceral and subcutaneous adipose tissue: similar levels but different associations with lipogenic and lipolytic genes. Am J Physiol Endocrinol Metab 299:E308–E317

28. World Health Organization (2000) Obesity: preventing and managing the global epidemic. Report of a WHO Consultation Geneva. WHO Tech Rep Ser 894. 1st ed. Geneva: World Health Organization.

29. International Diabetes Federation (2006) IDF consensus worldwide definition of the metabolic syndrome: www.idf.org/webdata/docs/MetS_def_update2006.pdf, accessed 24 November 2015.

30. Wabitsch M, Brenner RE, Melzner I, et al. (2001) Characterization of a human preadipocyte cell strain with high capacity for adipose differentiation. Int J Obes Relat Metab Disord 25:8-15

31. Fischer-Posovszky P, Newell FS, Wabitsch M, Tornqvist HE (2008) Human SGBS cells - a unique tool for studies of human fat cell biology. Obes Facts 1:184-189

32. Sembongi H, Miranda M, Han GS, et al. (2013) Distinct roles of the phosphatidate phosphatases lipin 1 and 2 during adipogenesis and lipid droplet biogenesis in 3T3-L1 cells. J Biol Chem 288:34502-34513

33. Sebastián D, Guitart M, García-Martínez C, et al. (2009) Novel role of FATP1 in mitochondrial fatty acid oxidation in skeletal muscle cells. J Lipid Res 50:1789-1799

34. Bradford MM (1976) A rapid and sensitive method for the quantitation of microgram quantities of protein utilizing the principle of protein-dye binding. Anal Biochem 72:248-254

35. Carman GM, Lin YP (1991) Phosphatidate phosphatase from yeast. Methods Enzymol 197:548-553

36. Han GS, Carman GM (2004) Assaying lipid phosphate phosphatase activities. Methods Mol Biol 284:209-216

37. Han GS, Carman GM (2010) Characterization of the human LPIN1-encoded phosphatidate phosphatase isoforms. J Biol Chem 285:14628-14638

38. Mul JD, Nadra K, Jagalur NB, et al. (2011) A hypomorphic mutation in Lpin1 induces progressively improving neuropathy and lipodystrophy in the rat. J Biol Chem 286:26781-26793

39. Cao H, Hegele RA (2002) Identification of single-nucleotide polymorphisms in the human LPIN1 gene. J Hum Genet 47:370-372

40. Fawcett KA, Grimsey N, Loos RJ, et al. (2008) Evaluating the role of LPIN1 variation in insulin resistance, body weight, and human lipodystrophy in U.K. Populations. Diabetes 57;2527-2533

41. Nye CK, Hanson RW, Kalhan SC. (2008) Glyceroneogenesis is the dominant pathway for triglyceride glycerol synthesis in vivo in the rat. J Biol Chem 283:27565-27574.

42. Csaki LS, Dwyer JR, Li X, et al. (2013) Lipin-1 and lipin-3 together determine adiposity in vivo. Mol Metab 3:145-154

43. Dwyer JR, Donkor J, Zhang P, et al. (2012) Mouse lipin-1 and lipin-2 cooperate to maintain glycerolipid homeostasis in liver and aging cerebellum. Proc Natl Acad Sci USA 109:E2486–E2495

44. Schweitzer GG, Chen Z, Gan C, et al. (2015) Liver-specific loss of lipin-1-mediated phosphatidic acid phosphatase activity does not mitigate intrahepatic TG accumulation in mice. J Lipid Res 56:848-858

45. Michot C, Mamoune A, Vamecq J, et al. (2013) Combination of lipid metabolism alterations and their sensitivity to inflammatory cytokines in human lipin-1-deficient myoblasts. Biochim Biophys Acta 1832:2103-2114

46. Banh T, Nelson DW, Gao Y, Huang TN, Yen MI, Yen CL (2015) Adult-onset deficiency of acyl CoA:monoacylglycerol acyltransferase 2 protects mice from diet-induced obesity and glucose intolerance. J Lipid Res 56:379-389

47. Mitra MS, Chen Z, Ren H, et al. (2013) Mice with an adipocyte-specific lipin 1 separation-of-function allele reveal unexpected roles for phosphatidic acid in metabolic regulation. Proc Natl Acad Sci USA 110:642-647

48. Choudhary V, Jacquier N, Schneiter R (2011) The topology of the triacylglycerol synthesizing enzyme Lro1 indicates that neutral lipids can be produced within the luminal compartment of the endoplasmatic reticulum: implications for the biogenesis of lipid droplets. Commun Integr Biol 4:781-784

Table 1 Correlation analysis in abdominal SAT and VAT adipose tissue biopsies from 71 participants

Variable	SAT			VAT		
	LPIN1	*LPIN2*	*LPIN3*	*LPIN1*	*LPIN2*	*LPIN3*
BMI	-0.349**	-0.021	0.220	-0.283†	-0.091	0.034
HOMA-IR	-0.471**	-0.104	-0.006	-0.329*	-0.139	-0.006
Glucose	-0.349**	0.253†	0.357**	-0.119	0.189	0.298†
Insulin	-0.522***	-0.169	-0.039	-0.340**	-0.179	0.017
Triacylglycerol	-0.319**	-0.018	0.072	-0.202	0.131	0.238
NEFA	-0.095	0.129	0.128	-0.029	0.125	0.336**
Glycerol	-0.188	-0.105	0.144	-0.113	0.097	0.274†

Spearman coefficient of the correlation analysis is shown. *p<0.05, **p<0.01, ***p<0.001
Where statistical power is lower than 80%: $^{\dagger}p$<0.01

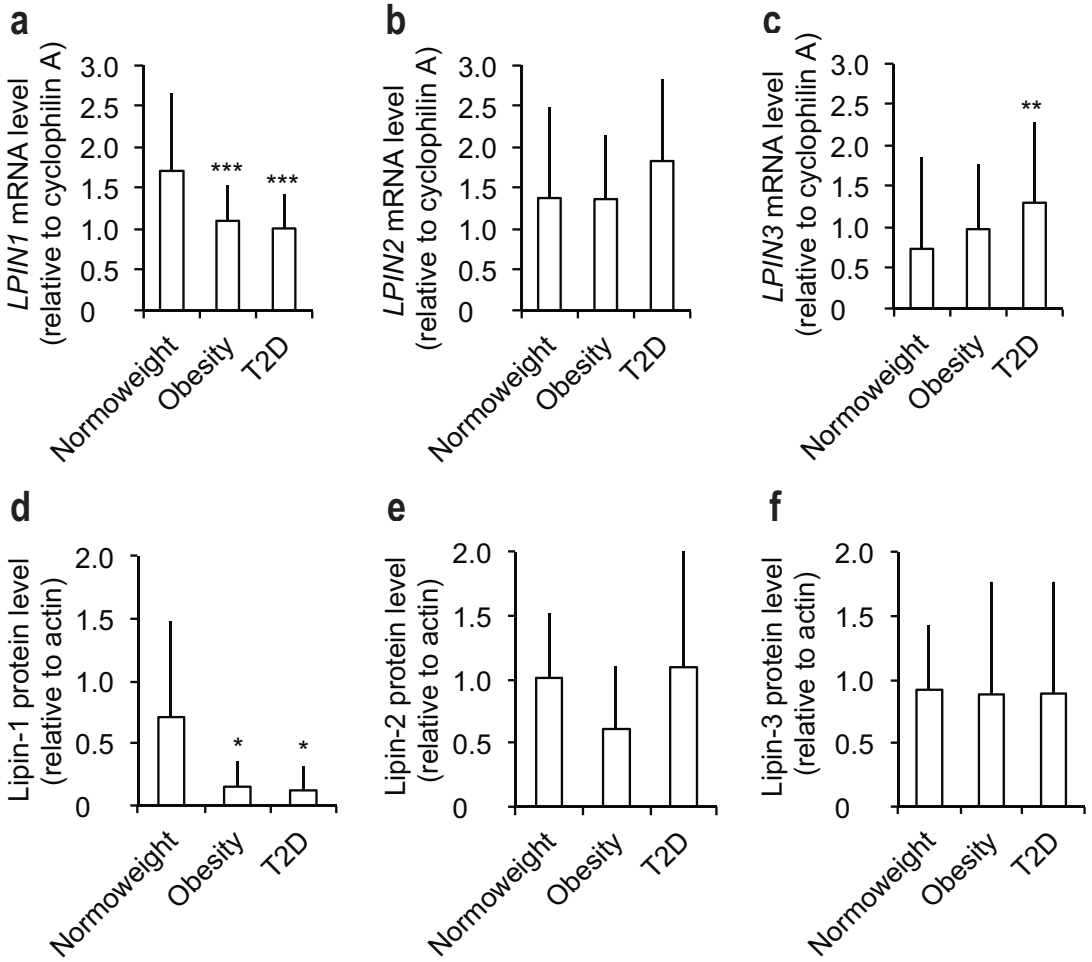

Fig. 1 Altered expression of the lipin family in type 2 diabetes adipose tissue. Participants were grouped by BMI and type 2 diabetes (T2D). (**a**–**c**) mRNA expression relative to cyclophilin A and to a calibrator that consisted of a mix of mRNA samples (n=17, 43 and 11), and (**d**–**f**) protein expression normalised to actin (n=9, 10 and 9) were quantified in human abdominal subcutaneous adipose tissue. Data represent mean ± SD; *p<0.05, **p<0.01, ***p<0.001 vs normoweight; ANOVA and Kruskal–Wallis tests

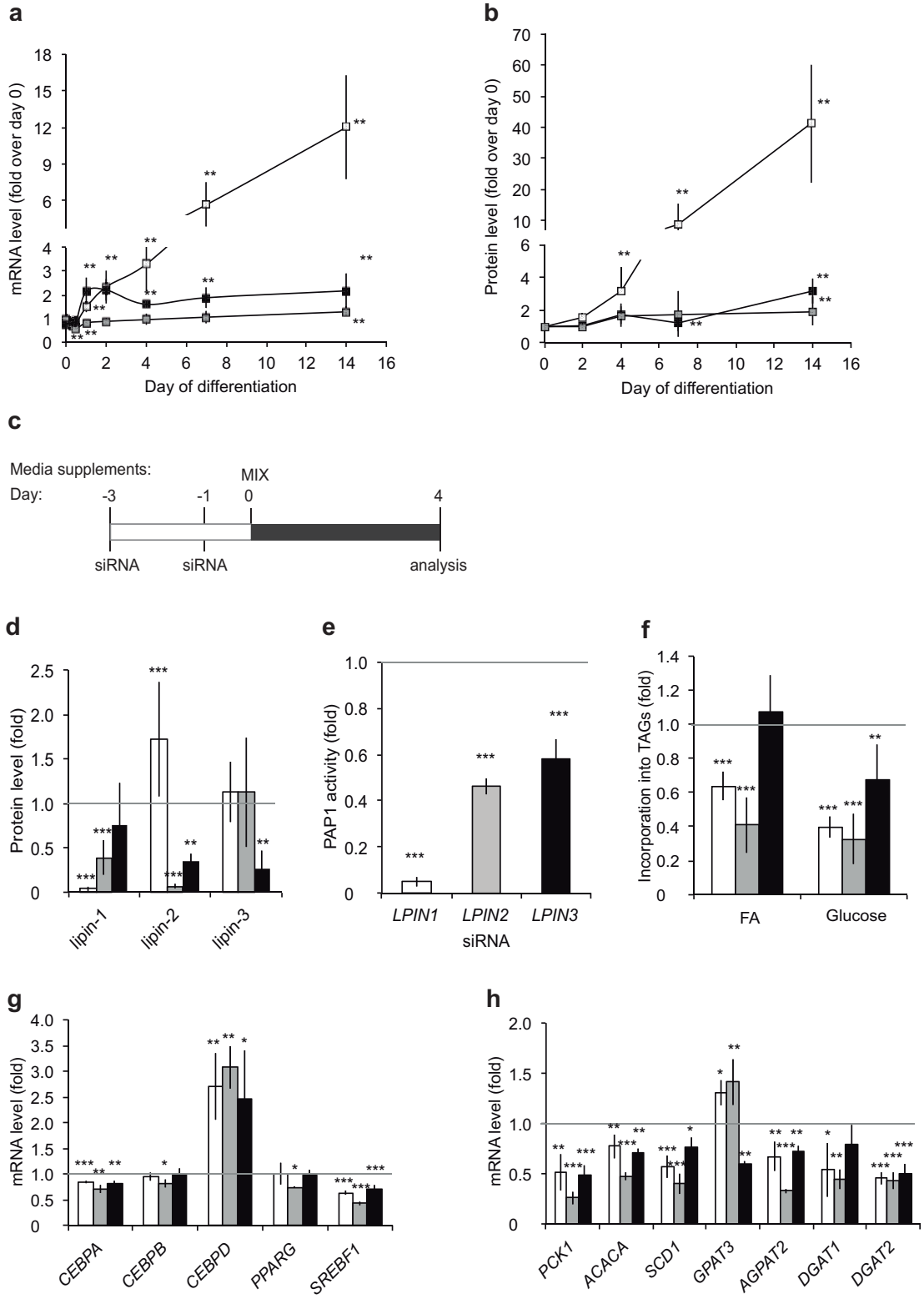

Fig. 2 Single knockdowns of lipins in SGBS pre-adipocytes. SGBS pre-adipocytes were induced to differentiate, and mRNA (**a**) and protein (**b**) levels were analysed during adipogenesis at the given time points (n=3). Data represent mean ± SD of fold induction over day 0. (**c**) Knockdowns of single lipin members were performed in pre-adipocytes, adipogenesis was induced (day 0) and cells were collected at day 4. (**d**) Lipin protein levels (n=7), (**e**) PAP1 activity (control: 23.10±5.12 nmol min^{-1} mg^{-1}) (n=3), (**f**) fatty acid (FA) and glucose incorporation into TAGs (control, fatty acids: 220.8±185.7 arbitrary units TAG/µg protein, glucose: 3.47±6.30 arbitrary units TAG/µg

protein) (n=3), and mRNA levels of (**g**) early adipogenic transcription factors (n=3), and (**h**) lipogenic genes (n=3) were analysed. Gene expression is expressed relative to cyclophilin 1A and to non-targeting control. Protein expression is normalised to actin levels. Data represent mean ± SD of fold increase over non-targeting controls (set as 1). *p<0.05, **p<0.01, ***p<0.001, General Lineal Model Univariate test. (**a**, **b**) White squares, *LPIN1*; grey squares, *LPIN2*; black squares, *LPIN3*; (**d**–**h**) white bars, *LPIN1* knockdown; grey bars, *LPIN2* knockdown; black bars, *LPIN3* knockdown

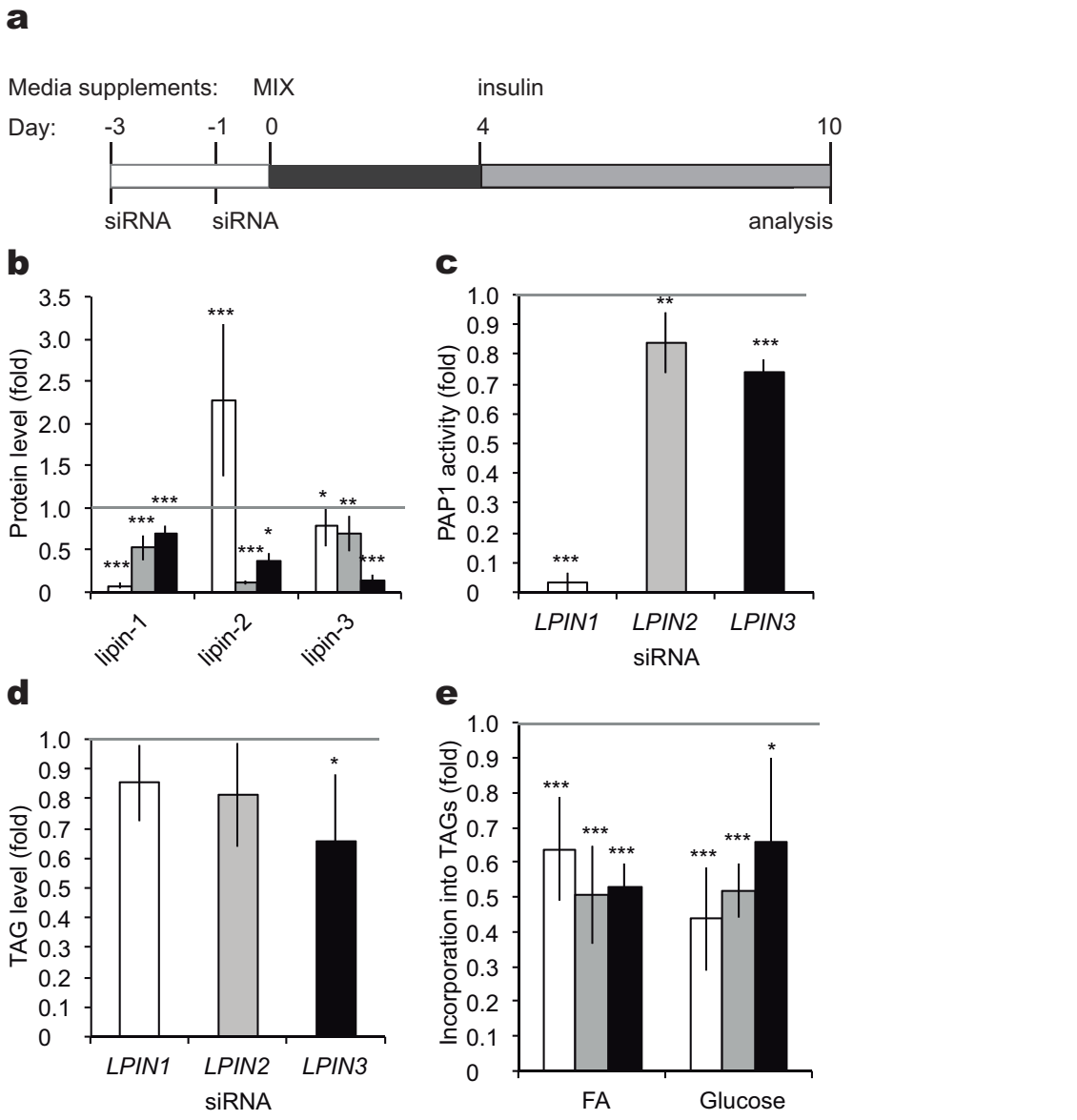

Fig. 3 Fully differentiation of lipin-depleted SGBS pre-adipocytes. (**a**) Knockdowns of single lipin members were performed in pre-adipocytes, adipogenesis was induced (day 0), and cells were collected at day 10. (**b**) Lipin protein levels (n=3), (**c**) PAP1 activity (control: 38.88±1.38 nmol min^{-1} mg^{-1}) (n=3), (**d**) total TAG content (control: 110.86±37.29 mmol l^{-1} mg^{-1}) (n=3), and (**e**) fatty acid (FA) and glucose incorporation into TAGs (control, fatty acids: 740.6±292.3 AU TAG/µg protein, glucose: 3.73±2.60 AU TAG/µg protein) (n=3) were analysed. Data represent mean ± SD of fold increase over non-targeting controls (set as 1); *p<0.05, **p<0.01, ***p<0.001; General Lineal Model Univariate test. White bars, *LPIN1* knockdown; grey bars, *LPIN2* knockdown; black bars, *LPIN3* knockdown

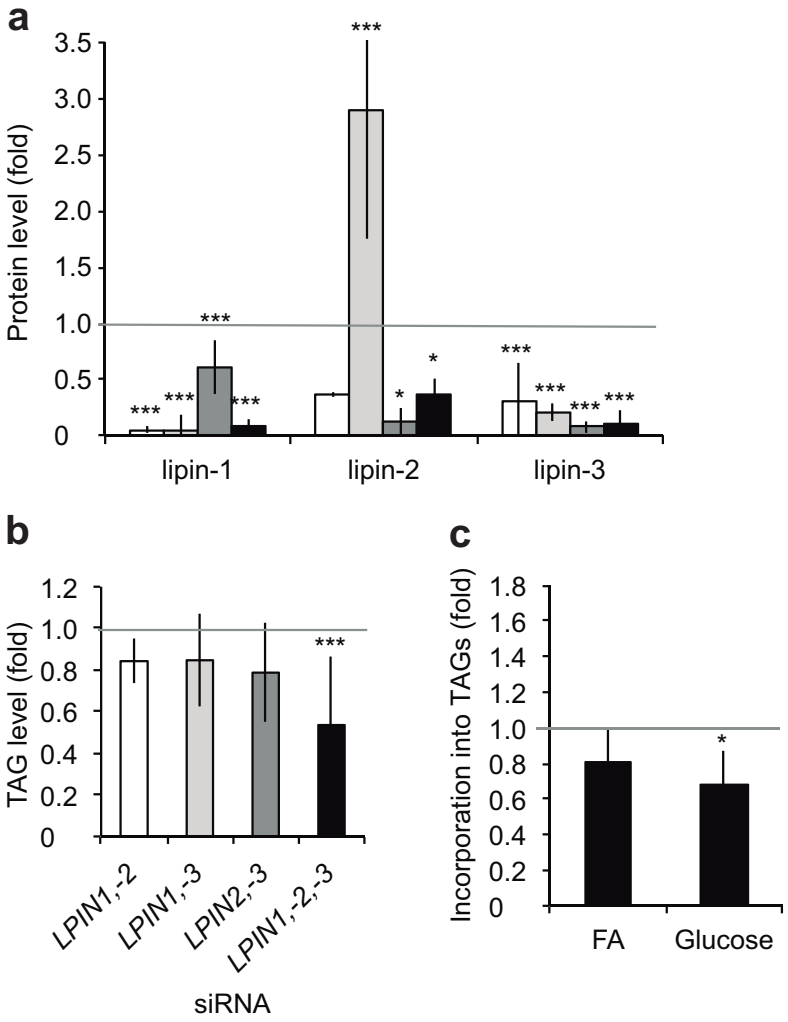

Fig. 4 Combinatorial depletion of lipins in SGBS pre-adipocytes after full differentiation. Multiple knockdowns of lipin members were performed in pre-adipocytes, adipogenesis was induced (day 0) and cells were collected at day 10. (**a**) Lipin protein levels (n=3–6), (**b**) total TAG content (controls: 71.11±36.40 and 101.79±76.15 mmol l^{-1} mg^{-1} for double and triple knockdowns, respectively) (n=5), and (**c**) fatty acid (FA) and glucose incorporation into TAGs in the triple knockdown (control, fatty acids: 493.4±226.4 arbitrary units TAG/μg protein, glucose: 3.51±2.26 arbitrary units TAG/μg protein) (n=3) were analysed. Data represent mean ± SD of fold increase over non-targeting controls (set as 1); *p<0.05, ***p<0.001; General Lineal Model Univariate test. White bars, *LPIN1* and *LPIN2* knockdown; light grey bars, *LPIN1* and *LPIN3* knockdown; dark grey bars, *LPIN2* and *LPIN3* knockdown; black bars, triple knockdown

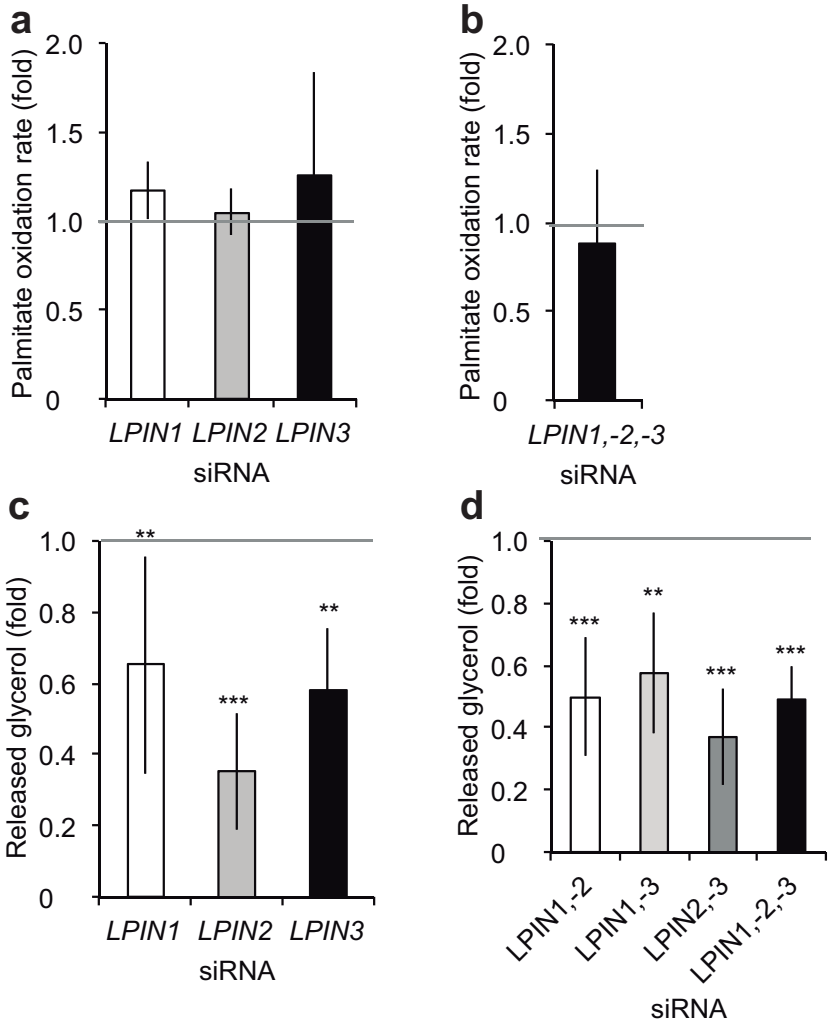

Fig. 5 Consumption of neutral lipids in fully differentiated lipin-depleted SGBS pre-adipocytes. Knockdown of single, double and triple lipin family members was performed in pre-adipocytes, adipogenesis was induced (day 0) and cells were collected at day 10. Palmitate oxidation rates in (**a**) single (control: 0.77±0.37 nmol h^{-1} mg^{-1}) (*n*=3), and (**b**) triple knockdowns (control: 0.63±0.28 nmol h^{-1} mg^{-1}) (*n*=3); glycerol release in (**c**) single (control: 0.42±0.12 mmol l^{-1} mg^{-1}) (*n*=3), and (**d**) combinatorial knockdowns (controls, double: 0.36±0.21, and triple: 0.21±0.07 mmol l^{-1} mg^{-1}) (*n*=5) were analysed. Data represent mean ± SD of fold increase over non-targeting controls (set as 1); $^{**}p<0.01$, $^{***}p<0.001$; General Lineal Model Univariate test. (**a**, **c**) White bars, *LPIN1* knockdown; grey bars, *LPIN2* knockdown; black bars, *LPIN3* knockdown; (**b**, **d**) white bars, *LPIN1* and *LPIN2* double knockdown; light grey bars, *LPIN1* and *LPIN3* double knockdown; dark grey bars, *LPIN2* and *LPIN3* double knockdown; black bars, triple knockdown

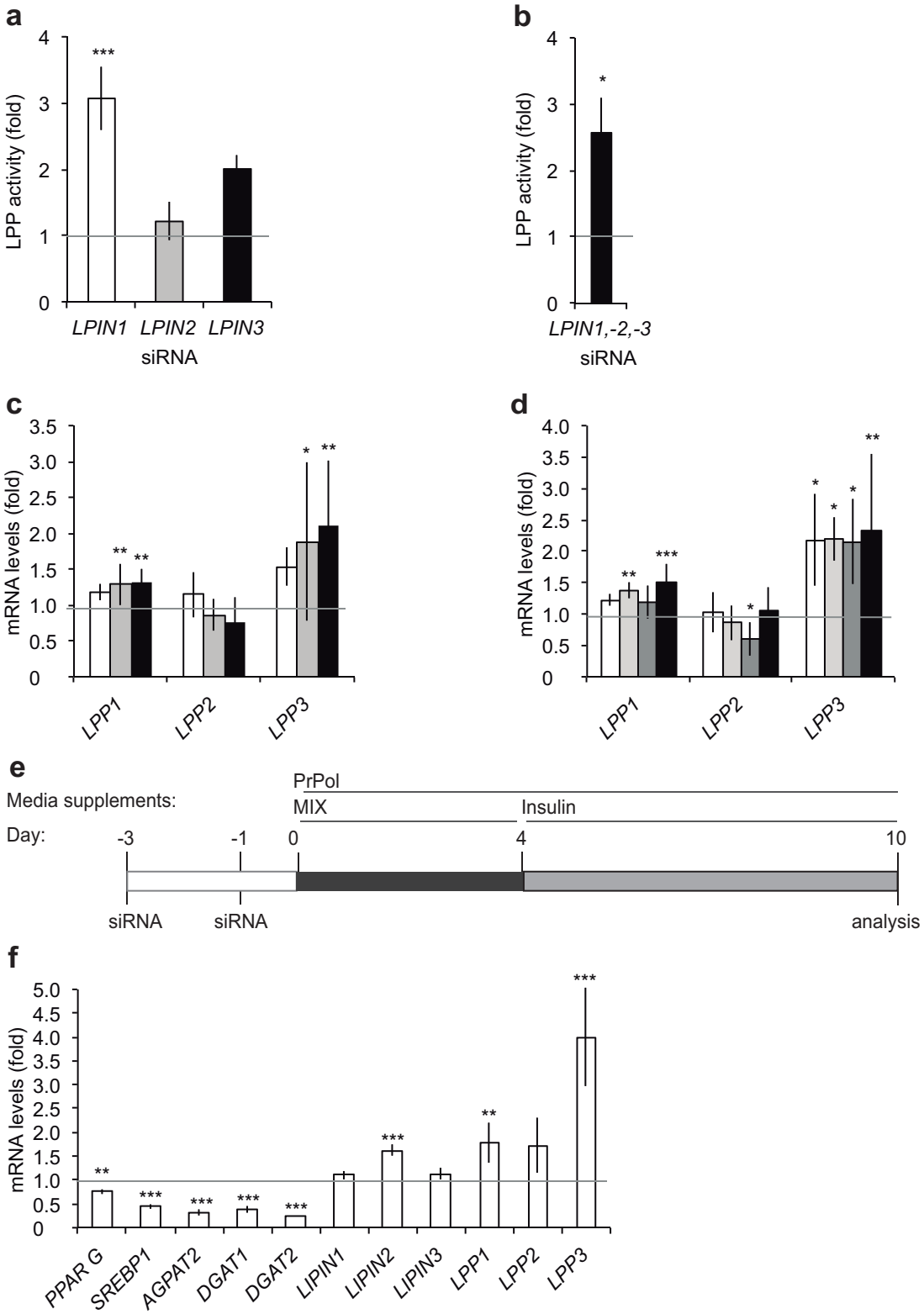

Fig. 6 Induction of the LPP family under conditions of repressed lipin expression. Knockdowns of single, double and triple lipin family members were performed in pre-adipocytes, adipogenesis was induced (day 0) and cells were collected at day 10. LPP activity in (**a**) the single (control: 6.01±0.60 nmol min^{-1} mg^{-1}) (*n*=3) and (**b**) triple knockdowns (control: 4.82±0.53 nmol min^{-1} mg^{-1}) (*n*=3), and expression levels of the LPP family in (**c**) the single (*n*=7) and (**d**) combinatorial knockdowns (*n*=4–7) were analysed. (**e**) SGBS pre-adipocytes were induced to differentiate in presence of 100

μmol/l of propranolol (PrPol). (**f**) mRNA levels of lipogenic genes were analysed (n=3). Data represent mean ± SD of fold increase over non-targeting controls (**a**–**d**) or non-treated control (**f**); *p<0.05, **p<0.01, ***p<0.001; General Lineal Model Univariate test. (**a**, **c**) White bars, *LPIN1* knockdown; grey bars, *LPIN2* knockdown; black bars, *LPIN3* knockdown; (**b**, **d**) white bars, *LPIN1* and *LPIN2* double knockdown; light grey bars, *LPIN1* and *LPIN3* double knockdown; dark grey bars, *LPIN2* and *LPIN3* double knockdown; black bars, triple knockdown; (**f**) white bars, propranolol

ESM Methods

Human adipose tissue biopy collection

Selection of patients— For the gene expression study, a group of 71 participants was recruited at Joan XXIII University Hospital (Tarragona, Spain) and Sant Pau i Santa Tecla Hospital (Tarragona, Spain). All participants were of Caucasian origin and reported that their body weight had been stable for at least 3 months before the study. They had no systemic disease other than obesity or type 2 diabetes, and all had been free of any infections in the month before the study. Liver and renal diseases were specifically excluded by biochemical workup.

The study included 17 normoweight, 43 individuals with obesity, and 11 individuals with type 2 diabetes, matched for age and gender (ESM Table 1A). Participants were classified by BMI according to the World Health Organization criteria [1]. Eleven patients were classified as having type 2 diabetes according to the American Diabetes Association criteria [2]. Variability in metabolic control was assessed by stable glycated haemoglobin A1c values during the previous 6 months. No patients were being treated with thiazolidinedione. Pharmacological treatment of the patients with type 2 diabetes was as follows: insulin, 9.1%; oral hypoglycaemic agents, 54.5%; statins, 63.6%; blood pressure- lowering agents, 54.5%.

Sample size was calculated, based in a previous study [3], to achieve a difference in normalized gene expression levels between the studied groups of 0.3 or greater with a confidence level of 95% and a statistical power of 80%.

Age and sex were assessed as interaction and confusing variables in the regression analysis. The global signification test was used to analyse interactions and for proposing the reference model. Residual analysis was performed to evaluate the models and data exclusion. The final regression model was chosen by comparing reduced models with the reference model.

For the protein expression levels of the lipin family, a group of 28 male participants was recruited at Joan XXIII University Hospital (Tarragona, Spain). The study included 9 normoweight, 10 individuals with obesity, and 9 individuals with type 2 diabetes, matched for age (ESM Table 1B).

Anthropometric measurements— Height was measured to the nearest 0.5 cm and body weight to the nearest 0.1 kg. BMI was calculated as weight (kilograms) divided by height (meters) squared. Waist circumference was measured midway between the lowest rib margin and the iliac crest.

Collection and processing of samples— VAT (omental) and SAT (anterior abdominal wall) samples were obtained from all individuals for the gene expression analysis, and SAT samples for the protein expression analysis. Samples were obtained during abdominal elective surgical procedures (cholecystectomy or surgery for abdominal hernia). All patients had fasted overnight. Blood samples were collected before the surgical procedure from the antecubital vein: 20 ml of blood with EDTA (1 mg/ml), and 10 ml of blood in silicone tubes. Fifteen millilitres of collected blood were used for the separation of plasma. Plasma and serum samples were stored at -80 C until analytical measurements were performed. Five millilitres of blood with EDTA were used to determine glycated haemoglobin A1c. Adipose tissue samples were collected, washed in 1X PBS, immediately frozen in liquid nitrogen, and stored at -80 C.

Analytical methods— Plasma glucose, cholesterol, and triacylglycerol levels were determined in an autoanalyzer (Hitachi 737; Roche Molecular Bio- chemicals, Marburg,

Germany) using the standard enzyme methods. High-density lipoprotein (HDL) cholesterol was quantified after precipitation with polyethylene glycol (PEG-6000) at room temperature. Non-esterified free fat acid (NEFA) serum levels were determined in an autoanalyzer (Advia 1200; Siemens AG, Munich, Germany) using an enzymatic method developed by Wako Chemicals (Neuss, Germany). Plasma glycerol levels were analyzed by using a free glycerol determination kit, a quantitative enzymatic determination assay (Sigma-Aldrich Corp., St. Louis, MO). Intra- and interassay coefficients of variation were less than 6% and less than 9.1%, respectively. Plasma insulin was determined by RIA (Coat-A-Count insulin; Diagnostic Products Corp., Los Angeles, CA) in all participants, except in insulin-treated type 2 diabetes patients. The homeostasis model assessment of insulin resistance (HOMA-IR) was determined as [glucose (mmol/l) x insulin (mIU/l)]/22.5 [4].

Cell culture and differentiation

Differentiation of SGBS cells— Preadipocytes were grown in serum-containing medium (DMEM/F12 supplemented with 10% foetal bovine serum, 33 µmol/l biotin, 17 µmol/l pantothenate and antibiotics) in a humidified 37 °C incubator with 5% CO_2, until reaching confluence. Cells were seeded at 25,000 cells per cm^2 and reached confluence in three days. To induce adipose differentiation cells were repeatedly washed with PBS buffer and cultured for four days in serum-free, basal medium supplemented with 33 µmol/l biotin, 17 µmol/l pantothenate, 1 nmol/l insulin, 200 pmol/l triiodothyronine, 0.1 µmol/l cortisol, 0.01 mg/ml transferrin, 0.5 mmol/l IBMX, 2 µmol/l rosiglitazone and 25 nmol/l dexamethasone (differentiation medium). Cells were cultured in adipocyte maintenance medium for one week (differentiation medium without IBMX, dexamethasone and rosiglitazone). The medium was changed twice a week.

Human adipose stem cell isolation—All tissues were obtained from patients undergoing elective liposuction surgery. Adipose-derived stem cells (ASC) were isolated from adipose tissue (n=3 female donors; age (years) 37.4±6.4, BMI (kg/m^2) 25.9±3.0), according to published protocols [5]. Briefly, ASC were obtained from washed lipoaspirate tissues by collagenase digestion as explained previously, from the Biobank of the Joan XXIII University Hospital. The resulting SVF cells were cultured in stromal medium consisting of Dulbecco's modified Eagle's medium (DMEM)/F12, 10% fetal bovine serum (FBS), plus antibiotics at 37 °C, 5% CO_2 overnight. The following day, the ASC were rinsed with warm PBS and maintained until 80–90% confluent. The ASC cultures were collected by trypsin digestion and aliquots of 10^6 cells cryopreserved in liquid nitrogen until required for experimentation.
Thawed ASC cells were transferred to culture vessels at a density of $5x10^3$ cells/cm^2 in preadipocyte medium (low glucose DMEM supplemented with 10% FBS, 15 mmol/l HEPES, 2.5 ng/ml Fibroblast growth factor-2, 33 µmol/l biotin, 17 µmol/l pantothenate and antibiotics). The cells were maintained in a humidified tissue culture incubator at 37 °C with 5% CO_2. The medium was replaced every second day until the cells reached 80% confluence. Cells were collected by trypsin digestion for inducing adipogenic differentiation.

Differentiation of ASCs— The ASCs were used at passage 5. To induce adipogenesis, confluent cultures of ASCs were cultured for 2 days in adipocyte differentiation medium (DMEM/F-12 supplemented with 10% FBS, 5 µmol/l rosiglitazone, 1 nmol/l dexamethasone, 0.5 mmol/l 1-methyl-3-isobutylxanthine (IBMX), 0.01 mg/ml transferrin, 1 nmol/l human insulin, 33 µmol/l biotin, 17 µmol/l pantothenate and

antibiotics). The induced cells were re-fed every 3 days with adipocyte maintenance medium (adipocyte differentiation medium without IBMX, and dexamethasone), during 12 days.

Quantification of expression levels

qPCR—Total RNA was extracted by using an RNeasy Lipid Tissue Midi Kit (total adipose tissue) and RNeasy Tissue Mini Kit (SGBS cells) (QIAGEN, Germantown, MD, USA). Total RNA was transcribed to cDNA by using a High-Capacity cDNA Reverse Transcription Kit (Applied Biosystems, LifeTechnologies Corporation). Real time qPCR analysis was performed with duplicates on a 7900HT Fast Real-Time PCR System using hydrolysis probes (Applied Biosystems, ESM Table 2C). SDS software 2.3 and RQ Manager 1.2 (Applied Biosystems) were used to analyse the results with the comparative quantification cycle (Cq) method ($2^{-\Delta\Delta Cq}$), and cyclophilin A as reference gene. For the human cohort analysis, samples from different groups were randomised at every qPCR run.

Western blot analysis— 10 μg of total protein per lane were resolved by electrophoresis in 8 to 12% SDS–PAGE, transferred to nitrocellulose membranes (Whatman), blocked in either 5% non-fat dry milk in PBS containing 0.01% Tween 20 or following manufacturer´s recommendations for 1 h at room temperature, incubated with the primary antibody overnight at 4 °C and secondary for 1 h. The western blots were developed with Super-Signal West Femto Maximum Sensitivity Substrate (Pierce). Images were quantified by using ImageJ v.1.48 (Wayne Rasband, National Institutes of Health, USA). Actin and GAPDH protein levels were used for normalisation.

Cell Fractionation

For cell fractionation, cells were processed as described previously [6], with some modifications. The whole process was performed in ice and centrifugations were performed at 16,000 x g and 4˚C. Mainly, SGBS cells were grown and differentiated in two wells from 6-well plates, washed with PBS, scrapped in 75 μl of 10 mmol/l Tris-HCl (pH 7.4), 0.2 mmol/l AEBSF, 1.5 mmol/l $MgCl_2$, 10 mmol/l NaCl, 0.5 mmol/l dithiothreitol (DTT). Lysed cells were incubated in ice for 15 minutes vortex mixed, and centrifuged 10 seconds. The supernatant was kept as cytosolic fraction and the pellet was resuspended in 20 mmol/l Tris-HCl (pH 7.4), 25% glycerol, 0.2 mmol/l AEBSF, 1.5 mmol/l $MgCl_2$, 420 mmol/l NaCl, 0.5 mmol/l DTT, 0.2 mmol/l EDTA. The lysate was incubated in ice for 20 minutes and centrifuged 2 minutes. The supernatant was kept as nuclear fraction and the pellet was resuspended in H_2O as membrane bound proteins.

Neutral lipid accumulation and metabolism

Fatty acid and glucose incorporation into TAGs was measured by incubating adipocytes for 16 h at 37°C in serum-free medium containing 0.5 mmol/l palmitate and 1 μCi/ml [1-14C] palmitate bound to 1% bovine serum albumin (BSA) or 5 mmol/l glucose and 1 μCi/ml [1-14C] glucose. Cells were then washed in PBS and lipids were extracted and separated by TLC to measure the incorporation of labelled fatty acid into TAGs, as described [7]. Data are expressed as arbitrary units normalizaed by protein content. For FAO analysis, adipocytes were washed in KRBH 0.1% BSA, preincubated at 37 ºC for 30 min in KRBH 1% BSA, and washed again in KRBH 0.1% BSA. Cells were then incubated for 4 h at 37 ºC with fresh KRBH containing 5 mmol/l glucose and 0.5 mmol/l carnitine plus 0.25 mmol/l palmitate and 1 μCi/ml [1-14C]palmitate bound to

1% BSA. Palmitate oxidation to CO_2 measurements were performed as previously described [7], and expressed as nmol of CO_2 h^{-1} mg^{-1} of protein.

Enzyme assay

The radioactive substrate [32P]phosphatidate was enzymatically synthesized from 1,2-dioleoyl-sn-glycerol and [γ-32P]ATP with Escherichia coli diacylglycerol kinase. PAP activity was measured with cell extracts at 37 C for 20 min in a total volume of 100 µl containing 50 mmol/l Tris-HCl (pH 7.5), 0.5 mmol/l MgCl2, 10 mmol/l 2-mercaptoethanol, 0.2 mmol/l [32P]phosphatidate (5,000 cpm/nmol), and 2 mmol/l Triton X-100.

Metabolomic analysis

SGBS cells were grown in 6-well plates, transfected with siRNA as explained above, and differentiated to day 4. Three wells from a 6-well plate were used per condition, and cells were washed with 1X phosphate buffer saline and collected by scrapping with 355 µl of methanol. Collected cells were sonicated, and an aliquot of 40 µl was used for protein quantification. The remaining volume was frozen and kept at -80 C until the analysis. Four replicas were performed.

Lipid extraction method— Lipids were extracted from lyophilized samples by adding 570 µl of a cold mixture of dichloromethane/methanol (2:1 v/v). The resulting suspension was vortexed and bath-sonicated for 5 min. We subsequently added 120 µl of cold water, vortex samples again and organic and aqueous layers were allowed to equilibrate for 10 min at room temperature. Cell lysates were centrifuged (15,000 rpm, 15 min at 4 C), and the organic phase (lipidic) was collected for drying under a stream of nitrogen. Lipid pellets were resuspended in 300 µl of acetonitrile/isopropanol/water (65:30:5 v/v) for LC-MS analysis. 100 µl of culture media was lyophilized and subsequently resuspended in dichloromethane/methanol (2:1 v/v) following the same procedure as that used for cells, with the exception that lipid pellets were resuspended in 200 µl (acetonitrile: isopropanol: water (65:30:5 v/v).

LC/MS analysis— Untargeted LC/MS analyses were performed using an UHPLC system (1200 series, Agilent Technologies) coupled to a 6550 ESI-QTOF MS (Agilent Technologies) operating in positive (ESI+) or negative (ESI–) electrospray ionization mode. Lipids were separated by reverse phase chromatography with an Acquity UPLC C8 column (150 x 2.1 mm, 1.8 µm). Mobile phase A = water/acetonitrile (60:40) (10 mmol/l ammonium formate and 0.1% formic acid) and B = isopropanol/acetonitrile (95:5) (10 mmol/l ammonium formate, 0.1% formic acid and 0.1% H2O). Solvent modifiers, such as 0.1% formic acid and 10 mmol/l ammonium formate, were used to enhance ionization, as well as to improve the LC resolution in both positive and negative ionization modes. The elution gradient started at 32% B (time 0–1 min), increased to 60% of B (time 1–4 min) and increased again to 100% B over 11 min (time 4–15 min). The injection volume was 2 µl for cell lipids and 5 µl for media lipids. ESI conditions: gas temperature, 150 C; drying gas, 13 l/min; nebulizer, 35 psig; fragmentor, 150 V; and skimmer, 65 V. The instrument was set to work over the m/z range 50–1200 with an acquisition rate of 3 spectra/sec. For compound identification, MS/MS analyses were performed in targeted mode, and the instrument set to acquire spectra over the m/z range 50–1000, with a default iso width (the width at half-maximum of the quadrupole mass bandpass used during MS/MS precursor isolation) of 4 m/z. The collision energy was fixed at 20 V.

Lipidomic data analysis— LC/MS (ESI+ and ESI− mode) data were processed using the XCMS [8] software to detect and align mzRT features. A feature is defined as a molecular entity with a unique m/z and a specific retention time. XCMS analysis of these data provided a matrix containing the retention time, m/z value, and integrated peak area of each feature for each sample of cells and culture medium. We constrained the initial number of features by means of the following criteria: only features above an intensity threshold of 3,400 counts were retained for further statistical analysis. Quality control samples (QCs) consisting of pooled cells from each condition were injected at the beginning and periodically every four samples. The performance of the LC/MS platform for each mzRT feature detected in the cell culture samples was assessed by calculating the relative standard deviation of these features on pooled samples (CVQC), following Vinaixa et al. [9]. Next, the intensities of the mzRT features were compared using a One-way ANOVA for each differentiation day separately, correcting for multiple testing using Tukey's 'Honest Significant Difference' method. Differentially regulated lipids (p value<0.05 and fold>2) were retained for further tandem MS characterization. Lipid structures were identified by matching tandem MS spectra against reference standards in HMDB [10], LIPIDMAPS [11] or LipidBlast [12] databases, or using CFM-ID software [13].

Abbreviations

(AEBSF) 4-(2-aminoethyl) benzenesulfonyl fluoride, (ASC) adipose-derived stem cells, (BSA) bovine serum albumin, (DTT) dithiothreitol, 1-methyl-3-isobutylxanthine (IBMX),

Bibliography

1. World Health Organization (2000) Obesity: preventing and managing the global epidemic. Report of a WHO Consultation Geneva. WHO Tech Rep Ser 894. 1st ed. Geneva: World Health Organization.
2. International Diabetes Federation (2006) IDF Consensus Worldwide Definition of the Metabolic Syndrome: https://www.idf.org/webdata/docs/MetS_def_update2006.pdf, accessed 24 November 2015.
3. Miranda M, Chacón MR, Gómez J, et al. Human subcutaneous adipose tissue LPIN1 expression in obesity, type 2 diabetes mellitus, and human immunodeficiency virus--associated lipodystrophy syndrome. Metabolism. 2007 Nov;56:1518-26.
4. Matthews DR, Hosker JP, Rudenski AS, Naylor BA, Treacher DF, Turner RC (1985) Homeostasis model assessment: insulin resistance and ß-cell function from fasting plasma glucose and insulin concentrations in man. Diabetologia 28:412–419
5. Pachón-Peña G, Yu G, Tucker A, et al (2011) Stromal stem cells from adipose tissue and bone marrow of age-matched female donors display distinct immunophenotypic profiles. J Cell Physiol 226:843-851
6. Andrews NC, Faller DV (1991) A rapid micropreparation technique for extraction of DNA-binding proteins from limiting numbers of mammalian cells. Nucleic Acids Res 19:2499.

7. Sebastián D, Guitart M, García-Martínez C, et al. (2009) Novel role of FATP1 in mitochondrial fatty acid oxidation in skeletal muscle cells. J Lipid Res 50:1789-1799
8. Smith CA, Want EJ, O'Maille G, Abagyan R, Siuzdak G (2006) XCMS: processing mass spectrometry data for metabolite profiling using nonlinear peak alignment, matching, and identification. Anal Chem 78:779-787
9. Vinaixa M, Samino S, Saez I, Duran J, Guinovart JJ, Yanes O (2012) A Guideline to Univariate Statistical Analysis for LC/MS-Based Untargeted Metabolomics-Derived Data. Metabolites 2:775-795
10. Wishart DS, Tzur D, Knox C, et al. (2007) HMDB: the Human Metabolome Database. Nucleic Acids Res 35:D521-526
11. Fahy E, Sud M, Cotter D, Subramaniam S (2007) LIPID MAPS online tools for lipid research. Nucleic Acids Res 35:W606-612
12. Kind T, Liu KH, Lee do Y, DeFelice B, Meissen JK, Fiehn O (2013) LipidBlast in silico tandem mass spectrometry database for lipid identification. Nat Methods 10:755-758
13. Allen F, Pon A, Wilson M, Greiner R, Wishart D (2014) CFM-ID: a web server for annotation, spectrum prediction and metabolite identification from tandem mass spectra. Nucleic Acids Res 42:W94-99

ESM Table 1. *Characteristics of the cohorts for the study of the mRNA (A) and protein (B) expression*.

A.	Normoweight	Obesity	T2DM
N	17	43	11
Age (yr) [mean (SD)]	53.88 ± 15.41	57.23 ±14.08	66.09± 8.58
Sex (N, Female)	12	25	5
BMI (kg/m^2) [median (IQR)]	23.81 (1.50)	27.99 (4.60)***	28.68 (3.53)***
HOMA-IR [median (IQR)]	0.82 (1.41)	1.22 (1.20)	3.66 (21.95)*
Glucose (mM) [median (IQR)]	4.74 (0.80)	5.53 (0.64)	8.33 (3.11)***
Insulin (µIU/mL) [median (IQR)]	3.57 (5.55)	4.49 (4.20)	10.23 (17.96)
Triacylglycerol (mM) [median (IQR)]	1.04 (0.87)	1.03 (0.76)	1.66 (1.08)
NEFA (mM) [mean (SD)]	1.00 ± 0.75	0.77 ± 0.26	0.92 ± 0.41
Glycerol (mM) [median (IQR)]	177.6 (239.1)	144.3 (132.4)	301.6 (255.8)*

B.	Normoweight	Obesity	T2DM
N	9	10	9
Age (yr) [mean (SD)]	51.67 ± 3.24	52.70 ± 4.24	55.22 ± 4.84
BMI (kg/m^2) [median (IQR)]	23.30 (3.91)	33.48 (5.32)***	35.22 (6.17)***
HOMA-IR [median (IQR)]	0.63 (1.38)	2.21 (3.08)	6.92 (7.30)**
Glucose (mM) [median (IQR)]	3.78 (1.11)	4.28 (1.67)	8.56 (4.82)**
Insulin (µIU/mL) [median (IQR)]	4.00 (5.03)	12.70 (12.21)	18.73 (12.32)**
Triecylglycerol (mM) [median (IQR)]	0.81 (0.82)	1.43 (1.25)	1.72 (1.60)*

Abdominal adipose tissue (AT) was extracted from a cohort of 71 and 28 subjects for the gene (A) and protein (B) expression analysis, respectively. Participants were grouped by BMI and type 2 diabetes (T2D). Clinical and anthropometrical variables were collected. Normal distributed data are expressed as mean value (SD), and for variables with no Gaussian distribution, values are expressed as median (interquartil range, IQR). *p<0.05, **p<0.01, ***p<0.001.

ESM Table 2. *Commercial reagents used in this study.*

A. siRNA OLIGONUCLEOTIDES

Symbol	Company	Reference
——————————— Silencer(R) Select Pre-designed siRNA ———————————		
LPIN1	Ambion	S23205, S23206
LPIN2	Ambion	S18590, S18591
LPIN3	Ambion	S35072, S35073
Non-Targeting control	Ambion	No. 1
——————————————— On-Target Plus siRNA ———————————————		
LPIN1	Dharmacon	J-017427-09, -11
LPIN2	Dharmacon	J-013458-09, -11
LPIN3	Dharmacon	J-032702-07, -08
Non-Targeting control	Dharmacon	D-001810-01

B. ANTIBODIES

Symbol	Company		Dilution
ACTIN	Sigma-Aldrich	A2228	1/1000
CALNEXIN	Abcam	ab22595	1/3000
GAPDH	Santa Cruz Biotechnology	sc-32233	1/400
PPARG	Cell Signaling	2443	1/1000
SREBP1c	Santa Cruz Biotechnology	sc-8984	1/1000
TUBULIN	Sigma-Aldrich	T6557	1/3000
——————————HRP-conjugated secondary antibodies against ——————————			
goat	Sigma-Aldrich	A8919	1/4000
mouse	Jackson Immunoresearch	115-035-008	1/7000
rabbit	Sigma-Aldrich	A0545	1/5000

C. HYDROLYSIS PROBES

Symbol	Gene	ID	CQ (mean ± SD) [a]
ACACA	acetyl-CoA carboxylase alpha	Hs01046047_m1	27.8 ± 0.4
AGPAT2	1-acylglycerol-3-phosphate O-acyltransferase 2	Hs00944961_m1	25.8 ± 1.6
CEBPA	CCAAT/enhancer binding protein (C/EBP), alpha	Hs00269972_s1	22.5 ± 1.3
CEBPB	CCAAT/enhancer binding protein (C/EBP), beta	Hs00270923_s1	22.5 ± 0.1#
CEBPD	CCAAT/enhancer binding protein (C/EBP), delta	Hs00270931_s1	29.4 ± 0.2#
DGAT1	diacylglycerol acyltransferase 1	Hs00201385_m1	26.6 ± 1.3
DGAT2	diacylglycerol acyltransferase 2	Hs00261438_m1	20.9 ± 0.6
GPAT3	glycerol-3-phosphate	Hs00262010_m1	26.8 ± 1.0

	acyltransferase 3		
LPIN1	lipin 1	Hs00299515_m1	23.2 ± 0.4
LPIN2	lipin 2	Hs00206237_m1	27.4 ± 0.3
LPIN3	lipin 3	Hs01040129_m1	25.0 ± 0.4
LPP1	phosphatidate phosphatase type 2A	Hs00170356_m1	23.0 ± 0.3
LPP2	phosphatidate phosphatase type 2C	Hs00186575_m1	28.4 ± 6.2
LPP3	phosphatidate phosphatase type 2B	Hs00170359_m1	25.7 ± 5.1
MOGAT1	monoacylglycerol O-acyltransferase 1	Hs00369695_m1	34.6 ± 1.8
MOGAT2	monoacylglycerol O-acyltransferase 2	Hs00228268_m1	34.6 ± 0.9
MOGAT3	monoacylglycerol O-acyltransferase 3	Hs00698325_m1	Non detectable
PCK1	phosphoenolpyruvate carboxykinase 1	Hs00159918_m1	20.4 ± 0.5
PPARG	peroxisome proliferator-activated receptor gamma	Hs00234592_m1	23.2 ± 0.4
PPIA	cyclophilin 1A	Hs99999904_m1	19.9 ± 0.5
SREBF1	sterol regulatory element binding transcription factor 1	Hs01088691_m1	22.1 ± 0.6

[a]mean CQ ± SD from the day 10-control (non-targeting siRNA control of single knockdowns), except #, which stands for day 4-control.

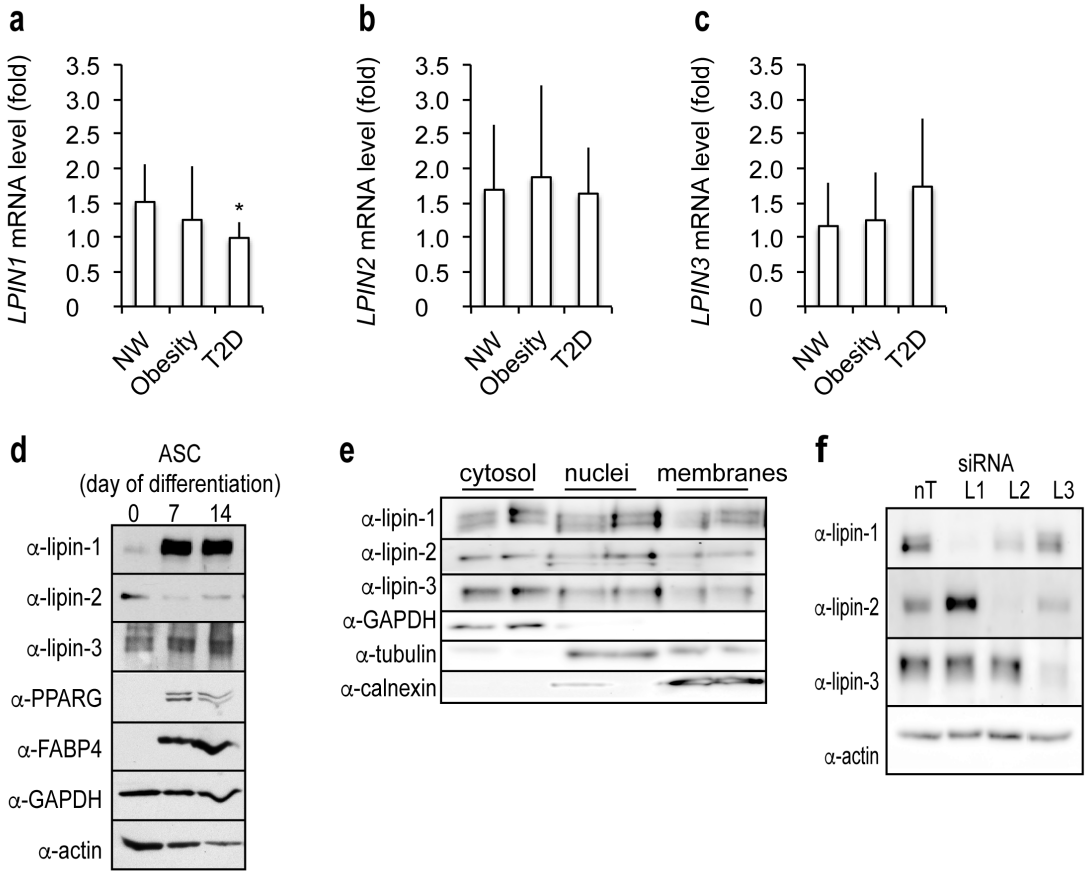

ESM Fig. 1. *Lipin expression levels in human adipocytes*. (a-c) Relative mRNA levels of the lipin family members were quantified in human abdominal visceral adipose tissue. Participants were grouped by BMI and type 2 diabetes (T2D). *, $p<0.05$ vs. normoweight; ANOVA and Kruskal-Wallis tests. (d) Protein levels of the lipin members were analysed during adipogenesis of adipose derived stem cells (ASC) from three different individuals. Protein levels of adipocyte markers (PPAR gamma and FABP4), and loading controls (glyceraldehyde-3-phosphate dehydrogenase (GAPDH), and actin), were also analysed. Portions of blots from a representative sample are shown. (e) Subcellular fractions containing cytosolic, intranuclear and membrane protein were isolated from SGBS adipocytes (day 10 after differentiation), and subcellular localization of endogenous lipin-1, -2 and -3 was assessed. Equal protein amounts from the fractions were loaded on an 8% SDS-PAGE and immunoblotted using the indicated antibodies. Markers for cytosol (GAPDH), nuclei (tubulin), and membranes (calnexin) were used. Representative portions of Western blots with duplicates are shown. (f) Single lipin-1, -2 or -3 knockdowns (L1, L2, or L3 respectively), and the non-targeting control (nT), were performed in SGBS preadipocyte cells. After induction of adipogenesis, cells were collected at day 4 and protein levels of lipins were analysed. Portions of blots from a representative sample are shown.

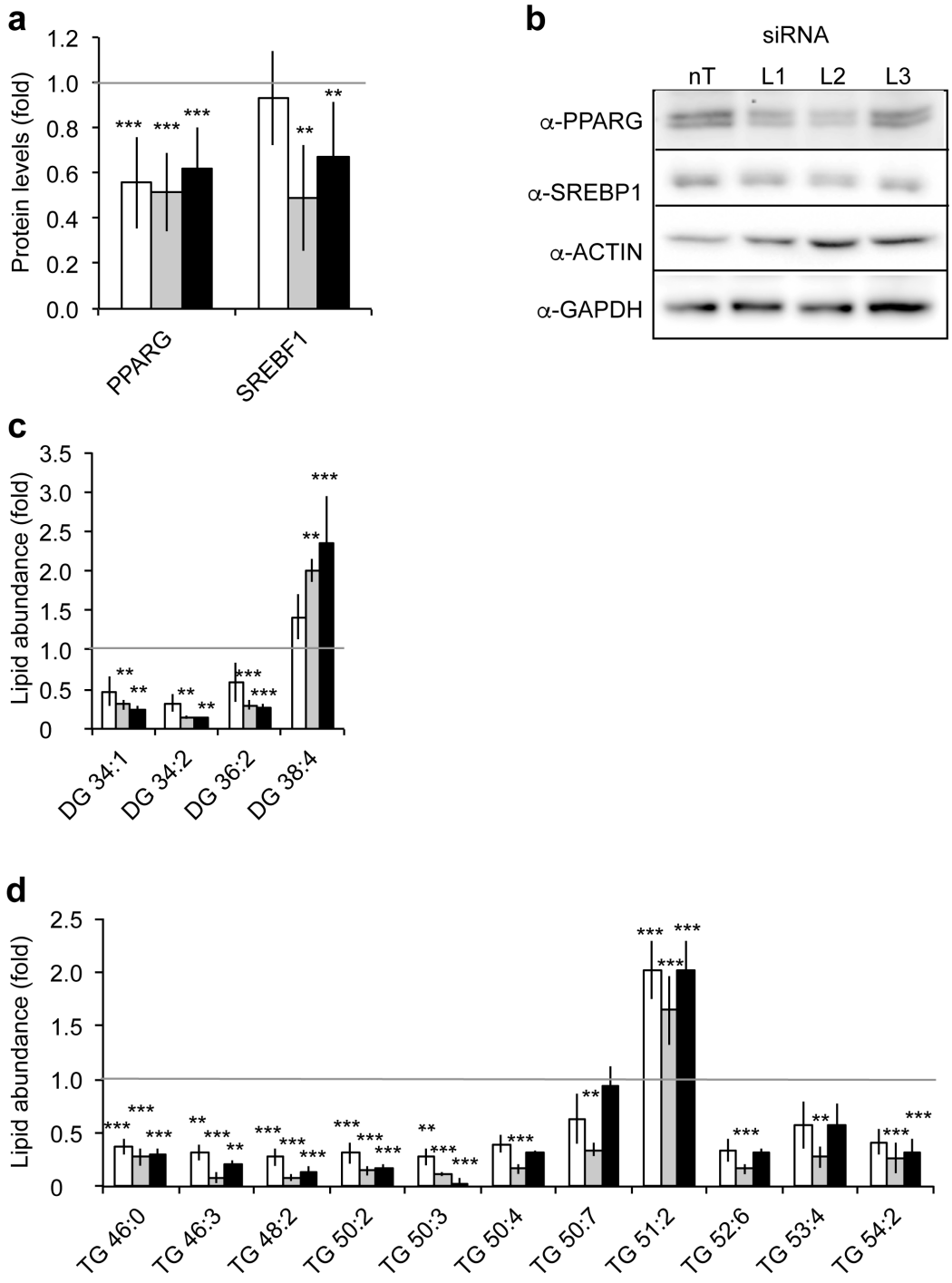

ESM Fig. 2. *The three members of the lipin family have a role in human SGBS lipogenesis in early adipogenesis stages*. Knockdowna of single lipin members were performed in SGBS preadipocyte cells. After induction of adipogenesis, cells were collected at day 4 and analysed. (a) Protein levels of transcription factors (n=7), and (b) representative portions of Western blots are shown. Abundance of significantly changed species of (c) diacylglycerol (DG) and (d) triacylglycerol (TG), (n=4). Data represent mean±SD of fold increase over non-targeting controls (set as 1). **p<0.01, ***p<0.001, General Lineal Model Univariate test. White bars, *LPIN1* knockdown; grey bars, *LPIN2* knockdown; black bars, *LPIN3* knockdown.

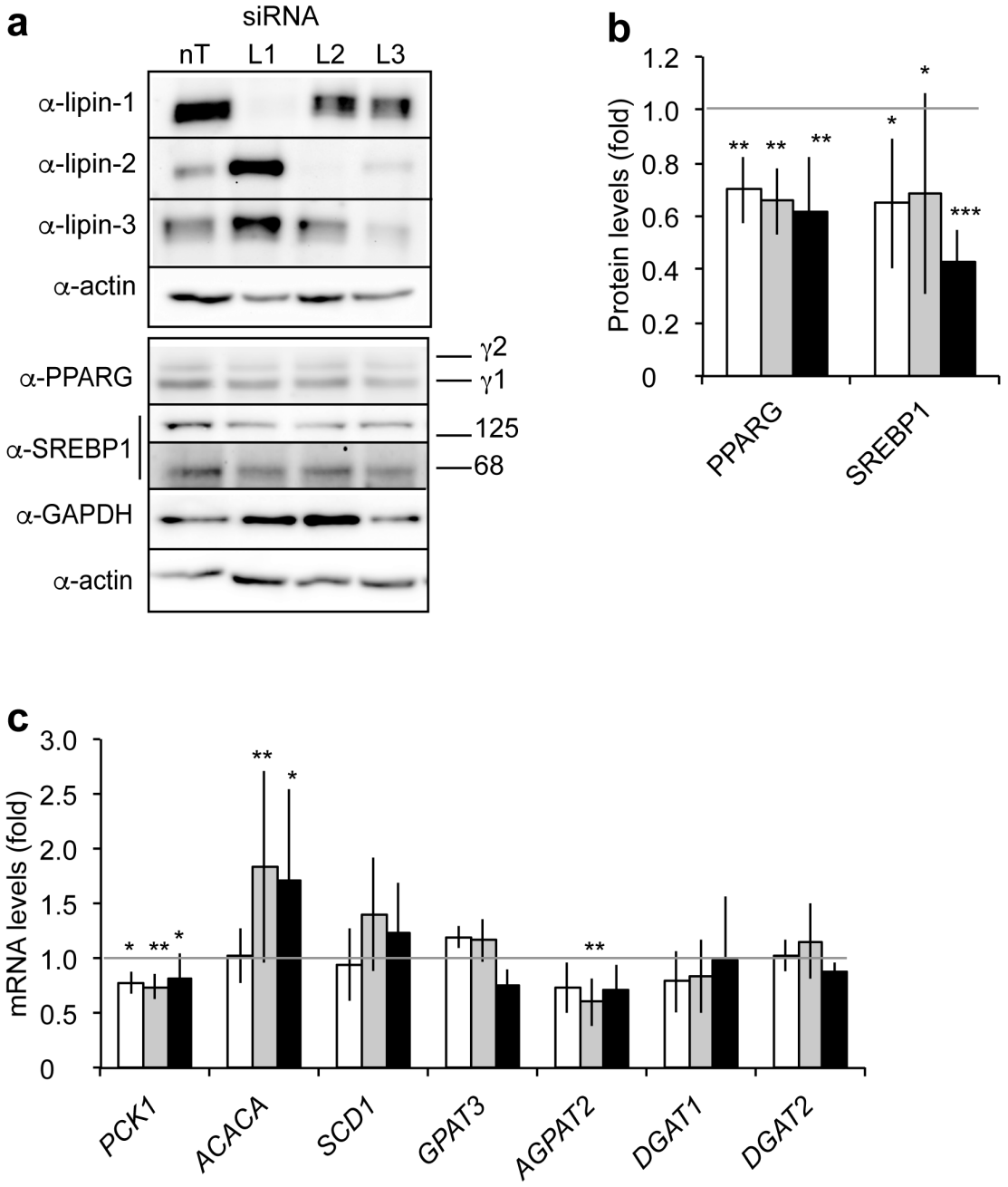

ESM Fig. 3. *Transcript and protein levels in lipin- depleted SGBS preadipocytes after fully differentiation.* Single knockdowns of lipin members were performed in SGBS preadipocyte cells. (a) At day 10 after differentiation, protein levels of the lipin family and adipocyte markers (PPAR gamma and SREBP1) were analysed. Portions of blots from a representative sample are shown. (b) Protein levels of transcription factors PPAR gamma and SREBP1 (n=5). (c) Transcript levels of genes involved in lipogenesis. Data represent mean±SD of fold increase over non-targeting controls (set as 1). *p<0.05, **p<0.01, ***p<0.001, General Lineal Model Univariate test. White bars, *LPIN1* knockdown; grey bars, *LPIN2* knockdown; black bars, *LPIN3* knockdown.

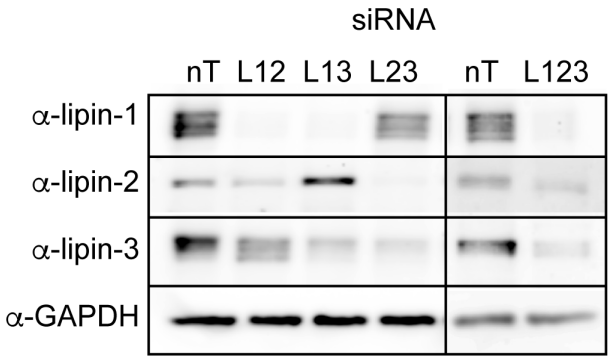

ESM Fig 4. *Combinatorial depletion of lipins in SGBS preadipocytes after fully differentiation. LPIN1* and *LPIN2* double knockdown (L12), *LPIN1* and *LPIN3* double knockdown (L13), *LPIN2* and *LPIN3* double knockdown (L23), triple knockdown (L123), and their corresponding non-targeting controls (nT), were performed in SGBS preadipocyte cells. Cells were induced to differentiate, and collected at day 10. Representative portions of Western blots are shown.

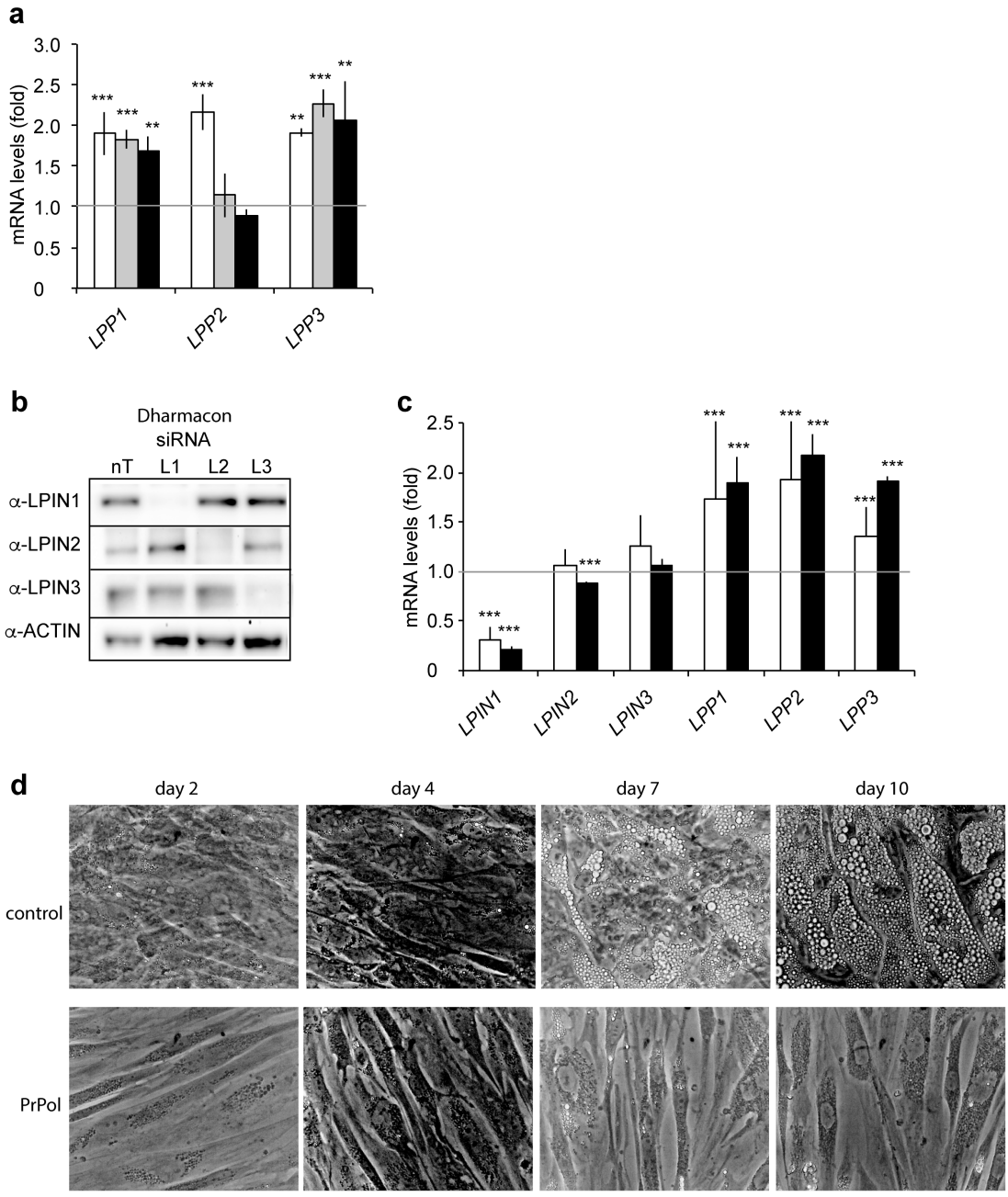

ESM Fig 5. *The LPP family is induced under conditions of repressed lipin expression.* Knockdown of single lipin members were performed in SGBS preadipocyte cells and cells were induced to differentiate. (a) Transcript levels of genes from the LPP/PAP2 family were analysed at day 4 after differentitation, relative to cyclophilin 1A and to control (n=3). (b, c) Single lipin knockdowns, and the corresponding non-targeting control, were performed in SGBS preadipocyte cells by using siRNA from two different sources and cells were collected on day 4 after differentiation. (b) Representative portions of Western blots of extracts from cells transfected with siRNA from Dharmacon (non targeting control, nT; single *LPIN1*, L1; *LPIN2*, L2; *LPIN3*, L3 knockdowns). (c) Transcript levels of cells transfected with *LPIN1* siRNA from both Dharmacon and Ambion were analysed (n=3-4). (d) SGBS preadipocytes were induced to differentiate in presence of 100 µmol/l propranolol (PrPol). Contrast-phase microscopy showed lipid droplet formation throughout adipogenesis is blocked in propranolol-treated cells. Data represent mean±SD of fold increase over non-

targeting controls (set as 1). **p<0.01, ***p<0.001, General Lineal Model Univariate test. (a) White bars, *LPIN1* knockdown; grey bars, *LPIN2* knockdown; black bars, *LPIN3* knockdown. (c) White bars, Dharmacon siRNAs; black bars, Ambion siRNAs.